metals

MDPI

Review

The Influence of Precipitation, High Levels of Al, Si, P and a Small B Addition on the Hot Ductility of TWIP and TRIP Assisted Steels: A Critical Review

Barrie Mintz * and Abdullah Qaban *

Department of Mechanical Engineering and Aeronautics, City, University of London, London EC1V 0HB, UK
* Correspondence: barriejenny9@gmail.com (B.M.); abdullah.qaban@city.ac.uk (A.Q.)

Abstract: The hot ductility of Transformation Induced Plasticity (TRIP) and Twinning Induced Plasticity (TWIP) steels is reviewed, concentrating on the likelihood of cracking occurring on continuous casting during the straightening operation. In this review, the influence of high levels of Al, Si, P, Mn and C on their hot ductility will be discussed as well as the important role B can play in improving their hot ductility. Of these elements, Al has the worst influence on ductility but a high Al addition is often needed in both TWIP and TRIP steels. AlN precipitates are formed often as thin coatings covering the austenite grain surfaces favouring intergranular failure and making them difficult to continuous cast without cracks forming. Furthermore, with TWIP steels the un-recrystallised austenite, which is the state the austenite is when straightening, suffers from excessive grain boundary sliding, so that the ductility often decreases with increasing temperature, resulting in the RA value being below that needed to avoid cracking on straightening. Fortunately, the addition of B can often be used to remedy the deleterious influence of AlN. The influence of precipitation hardeners (Nb, V and Ti based) in strengthening the room temperature yield strength of these TWIP steels and their influence on hot ductility is also discussed.

Keywords: TWIP; TRIP; Al; Si; P; Mn; S; C; Nb; V; Ti; B

Citation: Mintz, B.; Qaban, A. The Influence of Precipitation, High Levels of Al, Si, P and a Small B Addition on the Hot Ductility of TWIP and TRIP Assisted Steels: A Critical Review. *Metals* **2022**, *12*, 502. https://doi.org/10.3390/met12030502

Academic Editor: Marcello Cabibbo

Received: 28 January 2022
Accepted: 24 February 2022
Published: 16 March 2022

1. Introduction

TRIP (transformation induced plasticity) and TWIP (twinning induced plasticity) steels have a high strength combined with an excellent ductility [1–5], but their application has been disappointing considering their promising properties. In the case of TRIP steels, although their properties are better than DP (dual phase) steels, because of the easier processing route and the lower CEV (carbon equivalent value), the DP steels have been found to be more suitable for most applications, Table 1.

TRIP steel has higher C contents, (0.2–0.3% C) than DP steel (0.1–0.15% C) which makes spot welding of TRIP sheet steels more difficult in the automobile industry [6]. This is because of the rapid cooling induced after welding, which results in the formation of lower transformation products, leading to brittle failure [7].

Currently, TRIP-assisted steels are used in automobile structural components, longitudinal beams and B-pillar reinforcements and because they have higher n (strain hardening exponent) values and elongations than DP steels, in complex stampings. TRIP steels obtain their good room temperature properties by having present ~10% retained austenite (ϒ) in an essentially ferritic microstructure. This transforms to martensite under deformation and helps strengthen the steel and prevents "necking" down to failure, enabling very high elongations and strengths to be achieved [8]. For the automotive industry, high additions of Al and Si are often used to allow this ~10% retained austenite to form. This then results in a steel with a high strength combined with good ductility and press formability and so is very attractive for reducing the weight of vehicles so that less power is required to operate

them. The high additions of Al and or Si will also help to lighten, as well as strengthen, these TRIP steels.

Table 1. A comparison of mechanical properties of typical DP and TRIP steels with the same tensile strength [4] and TWIP 1000 with a higher tensile strength [5].

Steel	UTS MPa	YS MPa	Total Elong.%	Uniform Elong.%	n
DP800	825	440	18	17	0.13
TRIP800	831	503	28	21.5	0.24
TWIP1000	1009	464	>50	>45	0.42

UTS—Ultimate Tensile Strength, YS—Yield Strength, n—strain hardening exponent.

TWIP steels, in contrast, are fully austenitic and obtain their good properties by triggering the austenite to twin on deformation; the twin boundaries behaving like grain boundaries, strengthening the steel, resulting, again in both high strength and excellent ductility. TWIP steels have better properties than TRIP with a uniform elongation twice that of TRIP steel and a considerably higher ultimate strength and n value, Table 1 [2,5]. One of the problems with TWIP steels is that although their tensile strength is higher, than that of the TRIP steels, their yield strength for the same tensile strength is significantly lower, Table 1 (TWIP steels, are fully austenitic (face centered cubic—fcc) whilst TRIP steels, are mainly ferritic (bcc)) [5]. The properties of TWIP steel are superior to those of TRIP, but the high costs of the alloying elements (usually very high Mn levels, ≥15%Mn) and the difficulty of casting these high strength steels has limited their development.

A twin is formed under deformation by planes in the fcc austenite lattice shearing over each other, so that a hcp fault is formed, the lattice then returning to the fcc structure, as shown in Figure 1 [9].

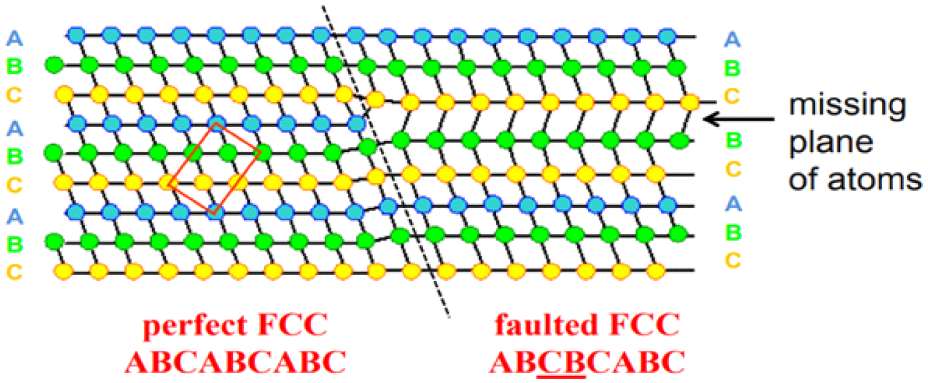

Figure 1. Schematic diagram showing the normal sequence of stacking (111) planes, ABCABCABC in the fcc crystal to that of missing out a plane so that the sequence changes to ABCBCABC, the stacking fault line being hcp [9].

To form this stacking fault, a certain amount of energy is required and if it is low, many twins can form on deformation. A stacking fault is generated on shearing by two partial dislocations separating and the energy is measured by the degree of separation [10]. If the energy is high the partial dislocations can only separate by a small distance and cross slip is favoured rather than twinning. On lowering the SFE (stacking fault energy), a stage is reached in which cross slip becomes difficult and twinning is favoured. However, if the SFE is too low, they are able to separate easily over a wide distance and a cross-slip is no longer possible, resulting in considerable work hardening, which causes the austenite to transform to martensite rather than a twin. Hence, twinning only occurs over a narrow SFE range, 20–40 mJ m^{-2} [11,12]. If the SFE is <2 0 mJ m^{-2}, work hardening is excessive and ε martensite forms [13,14] and if >40 mJ m^{-2}, normal glide takes place [11]. The SFE is

mainly dependent on the composition but the grain size of austenite and the deformation temperature are also important, coarsening the grain size leading to a lower SFE and increasing the temperature to a higher SFE [12].

However, before choosing a composition, as well as satisfying the SFE requirement to encourage twinning, it is also necessary to have a composition which is fully austenitic at room temperature. This is achieved by having a high Mn (15–25% Mn) and C content (0.4–0.6% C), so as to lower the Ms (martensite start temperature) below room temperature (all compositional percentages quoted in the paper are wt.%). Because of the overriding influence of C and Mn on the Ms, the following simple empirical equation is often used for these TWIP steels for obtaining a fully austenitic structure at room temperature [11]:

$$\%Mn + 13\%C \geq 17 \text{ to be fully austenitic} \quad (1)$$

This equation applies to TWIP steels with Mn contents of 15–30% and carbon contents of 0.1–0.8% [11]. This means that even with a low C level, it is still possible with a very high Mn level to obtain fully austenitic steels at room temperature, but because decreasing the C content lowers the SFE, the TWIP requirement may not be met [12].

In contrast, TRIP steels have much lower C contents (~0.2–0.3% C) and Mn contents (<2.5%Mn for δ TRIP) than the TWIP steels. In order to form a TRIP steel, a complex heat treatment is required: the steel is first heated to above the Ac1 (the lowest temperature at which austenite can form on heating at a specified heating rate) so that there is ~25% austenite present in the microstructure, stage (1) in Figure 2 [8]. Following this, the steel is rapidly cooled to ~400 °C so that the pearlite transformation is avoided and the ~25% austenite transforms partially to bainitic ferrite, stage (2) in Figure 2 [15]. The steel is then held at 400 °C for a short time, stage (3) in Figure 2. If ferrite formers such as Al, Si and P are present, the carbide transformation in the bainitic ferrite will be delayed, so the C content in the remaining austenite can be increased to over 1% before carbide precipitation takes place (stage (3). The steel before carbide precipitation commences is then cooled to room temperature producing a steel with ~10% stable retained austenite, (stage (4), Figure 2 [15].

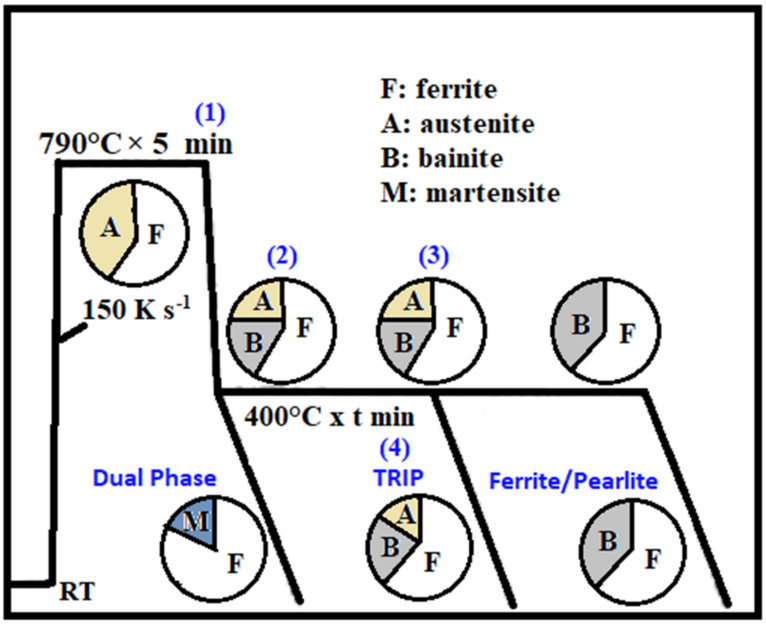

Figure 2. Mechanism of retained austenite formation during heat treatment of TRIP and DP steels [15].

Conventional TRIP steels use a high Si content (~1.5%) for the alloying addition, which delays carbide precipitation and allows the carbon to partition into the austenite rather than precipitating as a carbide in the bainitic ferrite [8]. However, for the automobile industry, galvanising is required to confer corrosion resistance and the presence of Si leads

to unsightly spots on the surface. High P additions will also delay carbide precipitation but again, can give rise to poor coatings on galvanising, which can delaminate from the steel surfaces [16]. Hence, Al additions have become a preferred addition for TRIP steels as strip steel can then be successfully galvanised, with no surface blemishes [8]. For the automotive industry, other advantages of the addition of elements like Al, Si and P is that they will lighten the vehicles, as well as strengthen the ferrite, being powerful solid solution hardeners.

2. Analysis of the Simple Hot Ductility Test for Evaluating the Likelihood of Cracking Occurrence on Straightening

The present review is concerned mainly with the hot ductility of these steels in relation to the ease of continuously casting them without cracking occurring in the straightening operation and follows previous reviews on the subject [17–19].

The continuous casting process is shown schematically in Figure 3 in which the strand is bent round from the vertical plane to the horizontal so that it can be cut into slabs of a suitable size for rolling to a thinner gauge. Unfortunately, the tensile stresses from this bending operation generate cracks on the top surface and edges of the strand in some grades of steel [17–19].

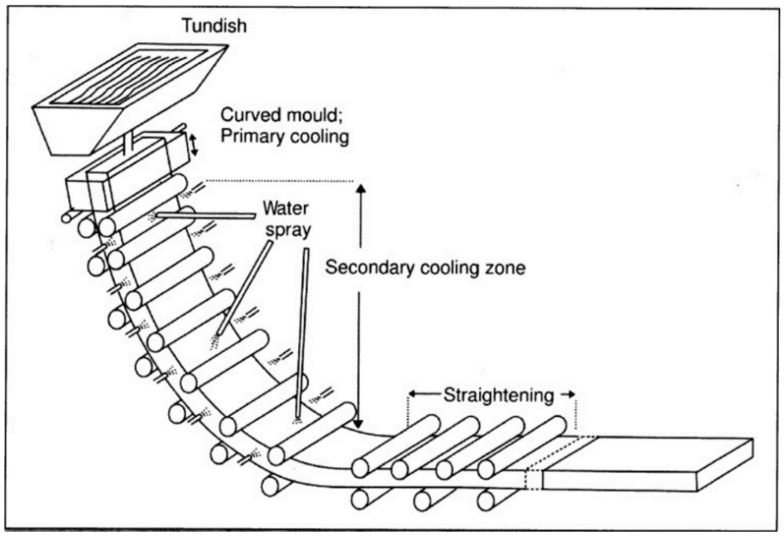

Figure 3. Schematic representation of a continuous casting machine.

A simple laboratory hot ductility tensile test has mainly, been used to assess the ductility needed to prevent cracking. This has proved to be successful in assessing the susceptibility to cracking of plain C-Mn, and HSLA (high strength low alloy) steels containing Nb and V. In the simple test, conditions are kept as close as possible to the continuous casting process [17]. The tensile sample is initially heated to 1250–1300 °C, which takes the microalloying elements back into solution and coarsens the austenite grain size to that reminiscent of the as-cast slab. The tensile specimen is then cooled at the average cooling rate undergone by the continuous cast slab as it cools from the melting point to the test temperature, which often is taken as 60 K/min and 200 K/min for thick (220 mm) and thin (40–60 mm) slab casting, respectively. The strain rate chosen for thick and thin slab casting is that applying during the unbending operation, ~10^{-3} s^{-1} and 10^{-2} s^{-1}, respectively [19]. The RA (reduction of area) value is then used as the measure of ductility.

Ti containing steels normally need to have the gauge length of the tensile specimen melted to take Ti (CN) back into solution but it is found even when incorporating this treatment into the testing procedure, there is little agreement between the commercial reality of Ti additions improving the hot ductility and results from the simple hot ductility test, which predicts the opposite [18]. This arises because one of the main faults associated with this simple test in an average cooling rate is chosen for the whole casting operation,

which as can be seen from Figure 4 is a much too simplified approximation of the cooling process undergone by the continuous cast slab [20].

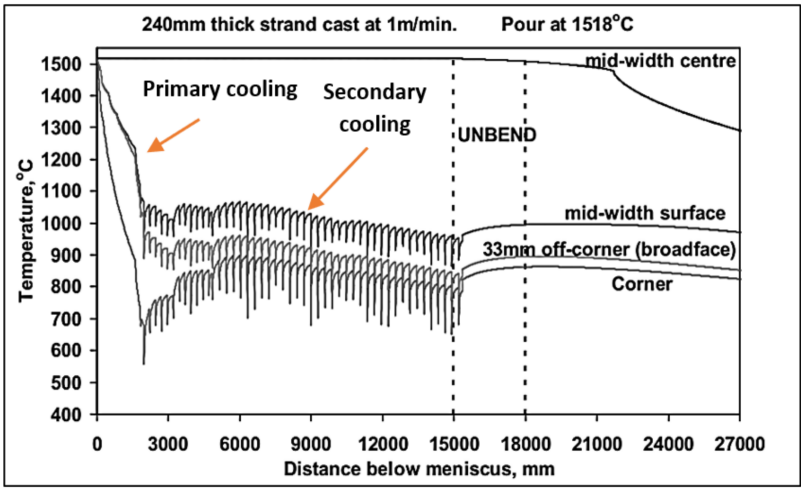

Figure 4. A 2-D computerised strand temperature model predicting the thermal history during continuous casting of a 240 mm thick strand cast at 1 m/min [20].

In the commercial operation, cooling is very rapid at the start of casting, reaches a minimum (primary cooling) and then rises, rapidly to a peak, followed by a slow progressive fall in temperature to the straightener (secondary cooling), Figures 3 and 4. During this secondary cooling the temperature of the slab cycles, increasing as it goes through guide rolls and decreasing again on exiting as the water sprays impinge on its surface, Figure 4. When after melting, both the average primary cooling rate and the average secondary cooling rate are incorporated into the laboratory test as in Figure 5, the ductility of Ti containing steels improves and there is then agreement between the commercial reality and laboratory predictions [20].

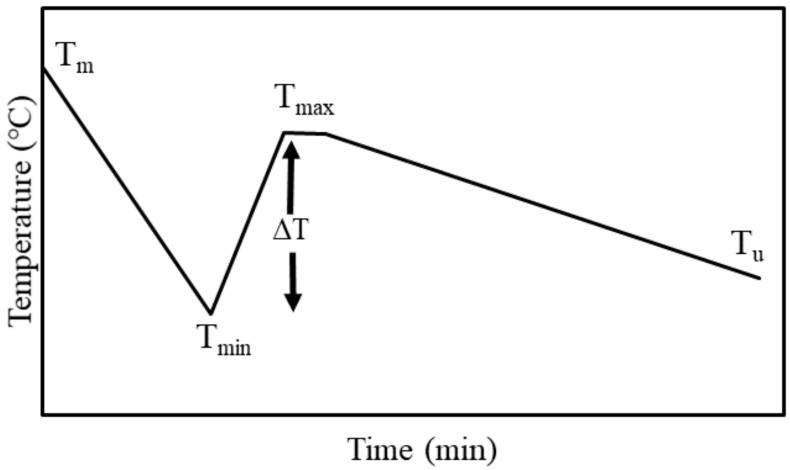

Figure 5. Thermal schedule used to generate the thermal condition of the billet surface in the continuous casting process: T_m is melting point, T_{min} and T_{max} are lowest and highest temperatures respectively. T_u is the temperature at the straightener and ΔT is the undercooling step [20].

The second major problem with the simple test is that it does not distinguish between the ductility of un-recrystallised austenite from that of recrystallised. During the straightening operation, no dynamic recrystallisation (DRX) is possible because the grain size is very coarse, ~500–1000 μm and the strain is very low (1–3%). This is in contrast to the tensile test, where with the very much higher strain, often >30%, DRX normally occurs at temperatures in excess of 800 °C [20]. An RA value of >35–40% is often taken as the criterion for good

ductility to avoid cracking on straightening but if this RA is due to DRX, this will not apply to the ductility required for the straightening operation [19]. Hence, when applying the RA values to assess the cracking susceptibility on straightening, the values obtained are only valid for the base of the trough and low temperature side of the hot ductility curve, not the high temperature side when DRX is possible [21].

The ductility for un-recrystallised austenite, as can be seen in Figure 6 [17], is very much lower (~50% RA) for the temperature range 800–900 °C than when fully recrystallised, >950 °C, (~80–100% RA). This piece of research work, Figure 6, represents one of the rare occasions when it has been possible to separate the ductility into the three components as shown in Figure 6, i.e., (a) ductility of the un-recrystallised austenite when the thin film of ferrite is present below Ae3 (the transformation temperature below which ferrite first starts to form under equilibrium conditions) and the Ar3 (the transformation temperature below which the steel first starts to form ferrite under non equilibrium conditions of cooling) in Figure 6, (b) ductility of the un-recrystallised fully austenitic structure (above the Ae3 in Figure 6) and (c) ductility when DRX of the austenite occurs (usually DRX occurs immediately after stage (1)). Only the first two components—(a) and (b)—are relevant to the straightening operation. The ductility of un-recrystallised austenite (the temperature range 800–900 °C in Figure 6 in which RA values are ~50%) can be seen to be higher than when the thin film of ferrite was present (temperature range 700–800 °C, ~40% RA) but only by a relatively small amount, ~10% RA. However, this improvement is often enough to avoid cracking. Nevertheless, although there is usually uncertainty with regards to the RA value of the un-recrystallised austenite, using a standardised testing regime for the tensile test it is found that, as long as the ductility at the base of the trough is ≥35–40% RA, there should be no cracking on straightening TRIP and HSLA steels, i.e., the ductility of the un-recrystallised steel above the Ae3 is unlikely to be lower than the 35–40% RA value criterion that is often taken as the value needed to avoid cracking [21].

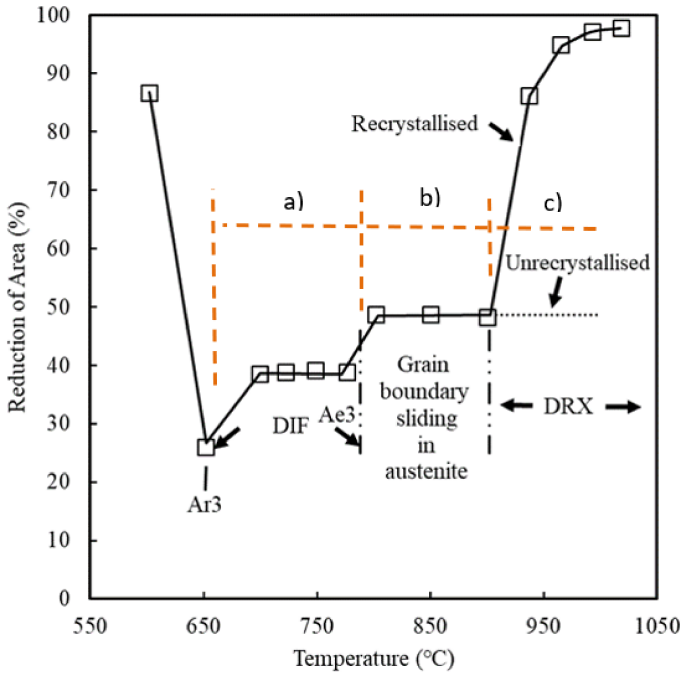

Figure 6. Hot ductility curve for a 0.4% C plain C-Mn steel tested at strain rate of 3×10^{-4} s^{-1} having no micro-alloying precipitates present showing all the different regions that are possible in the trough on cooling down through the austenitic temperature range, region (a) Deformation Induced ferrite (DIF) between Ae3 (the transformation temperature below which ferrite first starts to form under equilibrium conditions) and the Ar3 (the transformation temperature below which the steel first starts to form ferrite under non equilibrium conditions of cooling), region (b) Un-recrystallised γ, region (c) Recrystallised γ [17].

TWIP steels, in contrast to TRIP, are fully austenitic and so they do not have a hot ductility trough (i.e., as long as there is no fine dynamic precipitation in the straightening temperature range 700–1000 °C). However, they do, in contrast to TRIP steels, often have a problem of the ductility deteriorating with increase in temperature in the range 700–1000 °C making it difficult to cast without cracking [21].

3. Influence of Microstructure, Precipitation and Grain Size on the Hot Ductility of TRIP and TWIP Steels

For TRIP steels as with HSLA steels, the hot ductility is controlled very much by the presence of a thin film of deformation induced ferrite (DIF) which forms on the austenite grain surfaces at temperatures below the Ae3. This ferrite film is softer than the austenite grains it surrounds and on deformation most of the strain is concentrated there, leading to ductile intergranular failure, this being initiated by the MnS inclusions situated at the boundary. The DIF film often forms over a wide temperature range from the Ae3 to the Ar3 giving rise to a hot ductility trough, Figure 6. The presence of this film generally prevents DRX from taking place, DRX being easier when the film is no longer present at above the Ae3 [21]. Normally, when using the higher strain rate of ~10^{-3} s^{-1}, DRX occurs at approximately the Ae3 temperature so one does not have a region where the austenite is unrecrystallised. However, the very low strain rate used in Figure 6, 3×10^{-4} s^{-1}, causes DRX to occur at higher temperatures which are above the Ae3.

As well as MnS inclusions initiating ductile failure, precipitation both at the boundaries and within the matrix is also responsible for the intergranular failures. For steels which contain precipitation hardeners within the straightening temperature range, the hot ductility has been shown to depend mainly on the size of the precipitate and to a lesser extent on their volume fraction and whether they are situated in the boundaries or in the matrix. The relationship between the average particle size and RA value for Ti containing Nb and low Al steels is given in Figure 7 [19]. When the average particle size is less than 10–15 nm, ductility rapidly deteriorates and below 10 nm will not meet that required to avoid cracking. Above a particle size of 20 nm, further particle coarsening only has a small influence in improving the hot ductility. Finer particles in the austenite matrix increase the shear stress acting on the grain boundary and when they are also situated at the grain boundaries, enable cracks to grow and interlink more easily. This precipitation behaviour seems to apply equally to TRIP and TWIP steels [22], which perhaps is not surprising as it is the austenite phase that the precipitation is occurring in, for both steels.

However, the austenite grain size is also very important in controlling ductility. Coarser grains facilitate easier crack propagation along the boundaries. A typical relationship between grain size and the RA value is shown in Figure 8 for steels in which precipitation hardeners are absent [19,23]. When the grain size exceeds 400 μm, there is little further deterioration in the ductility. This again seems to apply equally to TRIP and TWIP steels, as can be seen from Figure 8 [23].

Increasing the strain rate generally improves ductility, as it reduces the time available for grain boundary sliding (GBS) [17]. However, there is little that can be done to alter this in the industrial straightening operation. The strain rate on straightening when thin slab casting is about 10 times faster than that for thick slab casting, but the better ductility from this increased strain rate is balanced by the worse ductility from the finer precipitation size formed by the faster cooling rate. Decreasing the cooling rate will generally improve ductility because it coarsens the precipitates [19].

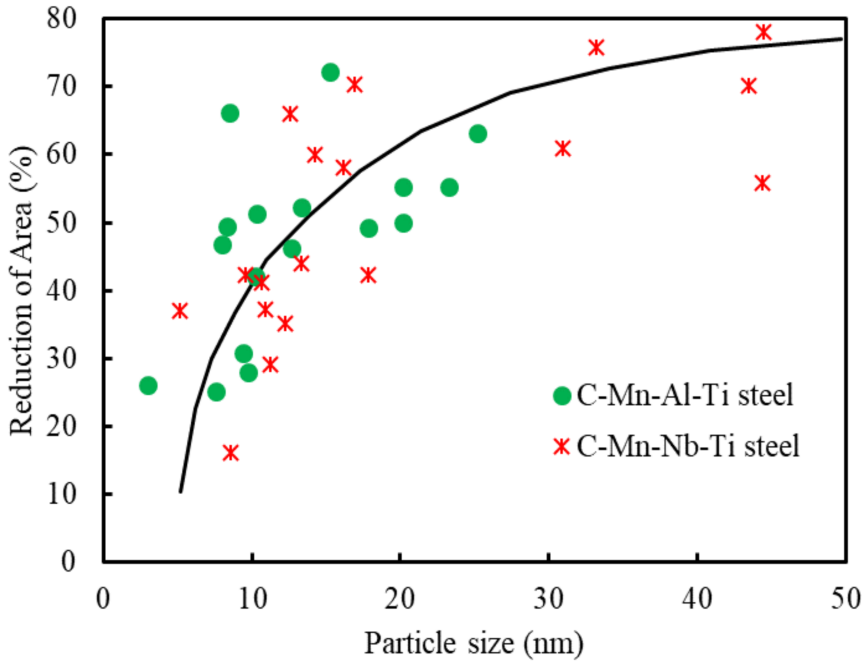

Figure 7. Influence of particle size on the RA value for C-Mn-Al-Ti and C-Mn-Nb-Al steels [19].

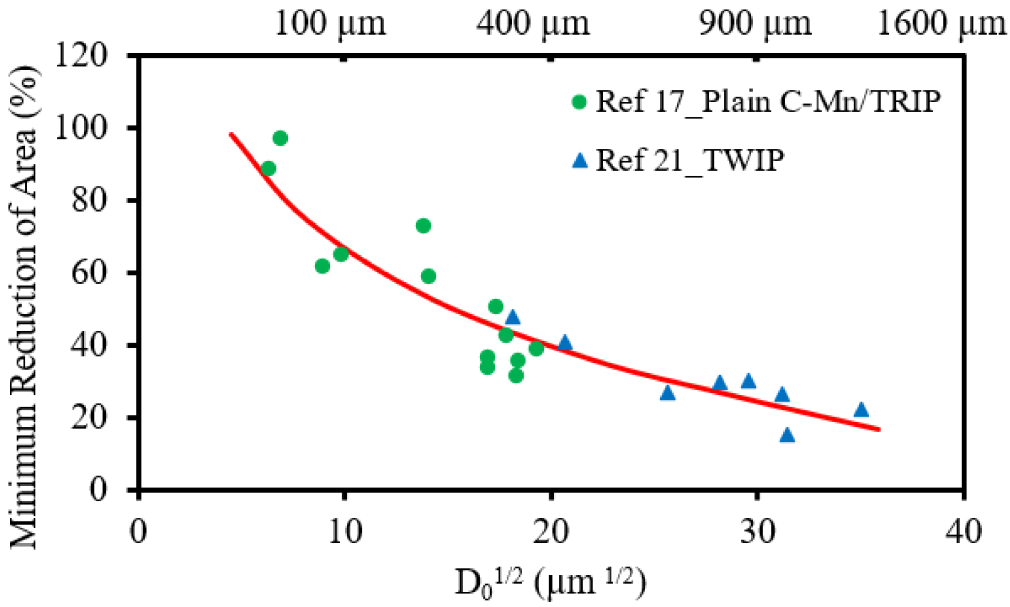

Figure 8. Influence of grain size on the RA value of steels, where D_o is the original grain size before deformation for steels having 0.15% C, 1.4% Mn in which precipitation hardening is not contributing to the RA value [17] and for TWIP steels having 0.6% C [21].

The shape of the hot ductility curve for these steels has been explained by a simple model, Figure 9a in which two curves are proposed, one of the fracture strain, ε_f against temperature, covering the temperature range when the thin film of ferrite is present; this strain being approximately constant over the temperature range of the trough and the other being the critical strain for dynamic recrystallization, ε_c against temperature [18]. Where the two curves intersect, TD is the temperature on cooling when the changeover occurs from DRX of the ϒ, to the presence of a thin film of deformation induced ferrite surrounding the unrecrystallised ϒ, Figure 9a. Increasing the strain rate causes both ε_c and ε_f to increase leading to a much narrower trough, Figure 9b. Refining the grain size, Figure 9c leads to an increase in ε_f and decrease in ε_c, again leading to a narrower trough [18] but the effect of

precipitation is to increase ε_c and decrease ε_f resulting in a very wide trough, Figure 9d. The Ae3 and Ar3 temperatures will always give good guidance as to the width of the trough.

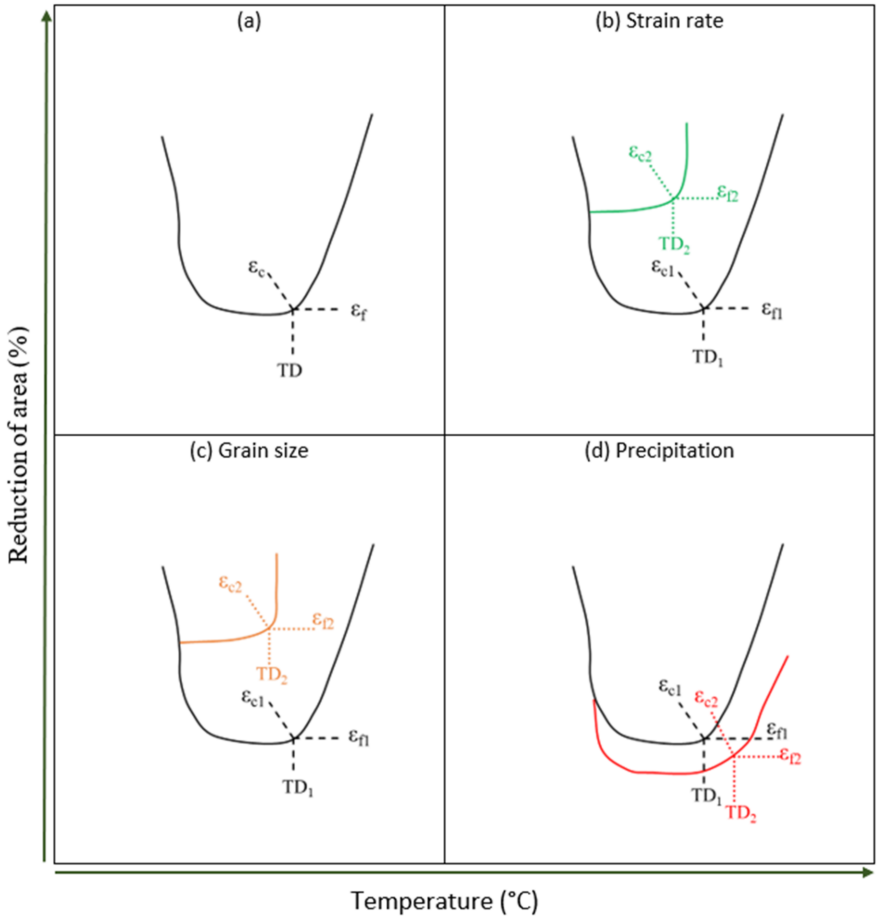

Figure 9. Schematic diagram showing (**a**) how the width of the ductility trough could be controlled by the dynamic recrystallization (DRX), (**b**) how increasing the strain rate reduces the depth and width of the trough where ε_{c1}, ε_{f1} and TD_1 refer to the lower strain rate. ε_{c2}, ε_{f2} and TD_2 refer to the higher strain rate (**c**) how refining the grain size reduces the depth and width of the trough, where ε_{c1}, ε_{f1} and TD_1 refer to the coarser grain size and ε_{c2}, ε_{f2} and TD_2 refer to the finer grain size and (**d**) the influence of precipitation in increasing depth and width of the trough where ε_{c1}, ε_{f1} and TD_1 refer to trough without precipitation and ε_{c2}, ε_{f2} and TD_2, the trough with precipitation. TD is the temperature on cooling when the changeover occurs from DRX of the γ, to the presence of a thin film of deformation induced ferrite surrounding the unrecrystallised γ.

4. Influence of High Al on the TRIP and TWIP Steels

High Al additions are often needed in both TRIP and TWIP steels for a variety of reasons. Al additions at the 1–1.5% level will prevent hydrogen cracking for both the steels, this being a serious problem with high strength steels, Figure 10 [5,24]. One of the original worries with having a high Al addition was whether the aluminium oxide formed during casting would tend to clog up the nozzles during pouring but this has fortunately not been the industrial experience and there is a thermodynamic analysis which confirms that this should not happen [25].

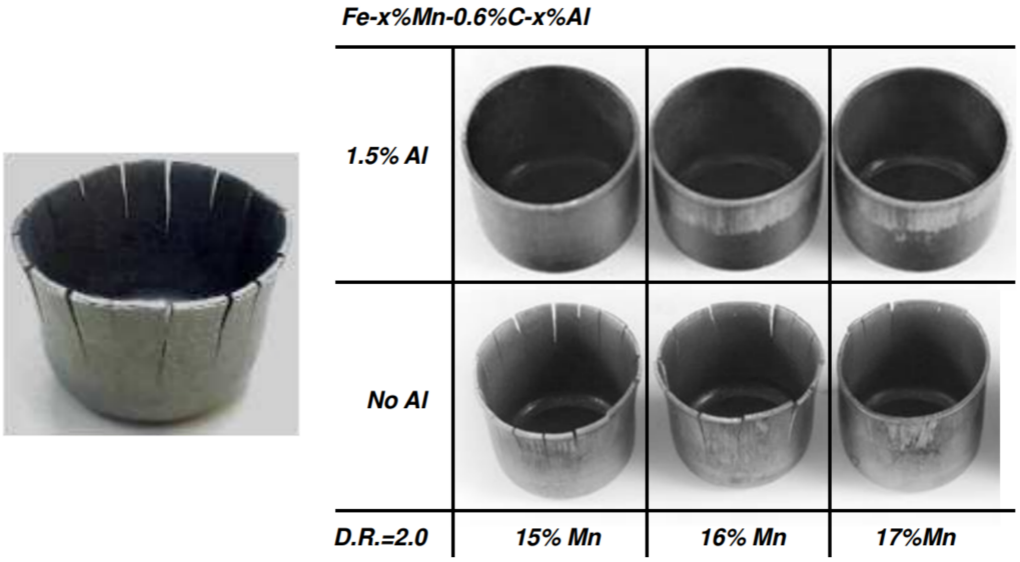

Figure 10. Example of delayed fracture in a deep drawn Fe-22% Mn-0.6% C, TWIP steel cup (top, left). Right, Top row: Suppression of delayed fracture by 1.5% Al addition in deep drawn Fe-xMn-0.6% C, TWIP steel cups having 15, 16 and 17% Mn. Right, bottom row: Cups showing cracks in the same steels without an Al addition due to delayed fracture [5].

In the case of TRIP steels, as mentioned a high Al addition prevents carbide precipitation in ferritic bainite ensuring that the carbon content of the retained austenite is high (~1% C), so that it is stable at room temperature and will transform to martensite on deformation but also importantly, it does not cause unsightly blemishes when the strip steel is galvanised for use in the automotive industry.

For TWIP steels, a high Al content will help balance the SFE so that it falls into the required range for twinning to occur but also that it strongly depresses the Υ to ε martensite transformation, encouraging twinning [14].

The present review is concerned mainly with the hot ductility and here there is a big problem with adding a high Al addition. Of all the microalloying additions (taking AlN here, as a microalloying addition), Al is the worst as it precipitates preferentially at the austenite grain boundaries as AlN and this weakens the boundary, favouring intergranular failure as well as stunting DRX. It can often precipitate as a thin coating over the dendritic boundaries Figure 11a,b [26,27] or in a very coarse form along the austenite grain boundaries, Figure 11c and both forms are very detrimental to ductility.

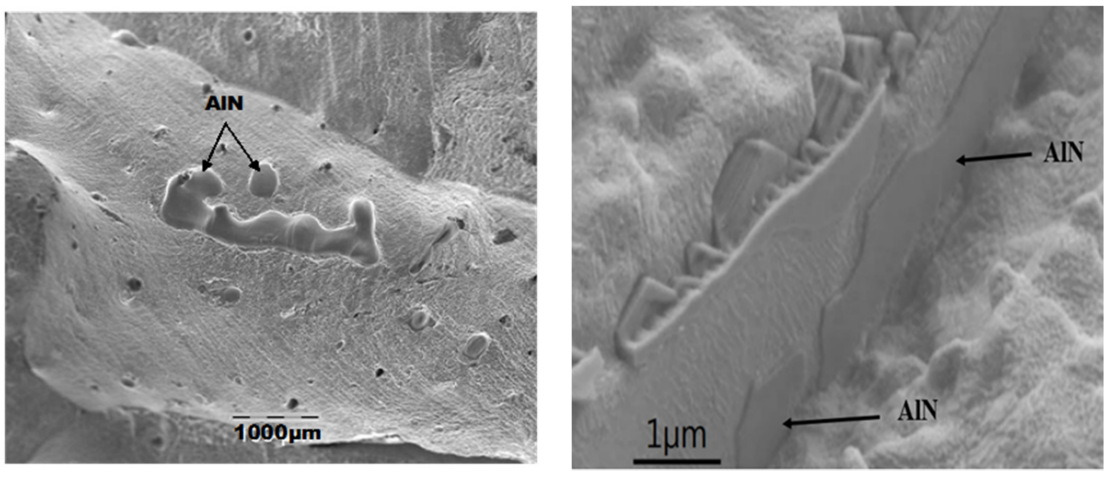

(**a**) (**b**)

Figure 11. *Cont.*

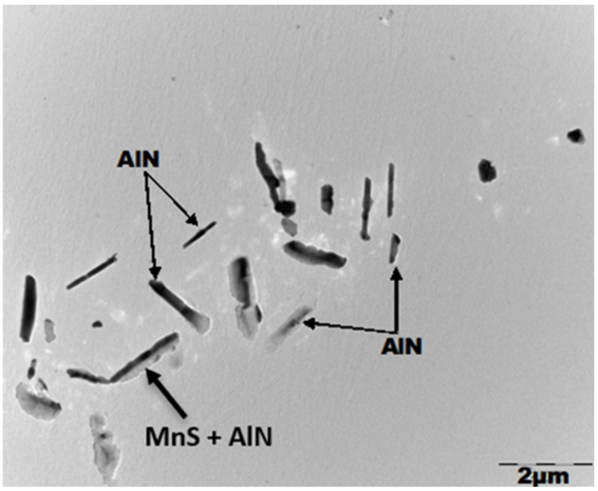

(**c**)

Figure 11. Various forms of AlN precipitation at the boundaries in as-cast high Al, TWIP steels (0.6% C, 18% Mn). Thin films of AlN on the dendritic surface of a high Al, TWIP steel (**a**) 1.6% Al, 0.007% N, (**b**) 1.4% Al, 0.004% N and very low S, 0.002% S (**c**) Very coarse AlN precipitates situated at the austenite grain boundaries [26,27].

The detrimental influence of AlN on hot ductility has not always been appreciated when it precipitates because of the practical difficulty of locating this thin coating of AlN at the grain surfaces. Generally, for low N (0.005%), steels of peritectic C content up to 0.04% Al can be present before ductility is adversely affected. Tuling et al. could not find after an extensive SEM-FDG electron microscope examination, any AlN precipitation in an as-cast 0.15% C, 2.45% Mn, 0.025% Nb TRIP steel tensile specimen having present 0.05% Al and 0.007% N [28]. This probably arises because of the sluggishness of AlN precipitation [29] and means it either does not precipitate at all in the time of the tensile test or too little is precipitated out to influence hot ductility. However, certainly when as much as 1% Al is added to TWIP and TRIP steels, profuse precipitation of AlN occurs at the boundaries and ductility deteriorates giving "rock candy" type fractures, Figure 12 [28]. Hence, these steels are very difficult to cast without cracks forming on straightening. This type of failure, "rock candy" does not occur with low Al (<0.4% Al) containing microalloyed even though intergranular fracture, not related to AlN precipitation does take place and shows how detrimental having a waver thin film of AlN can be.

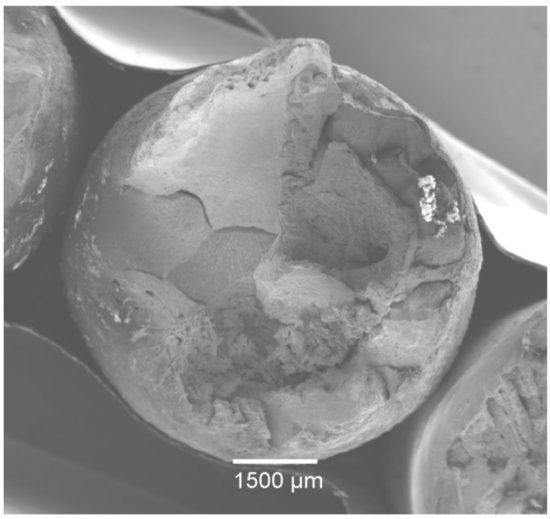

Figure 12. "Rock candy" fracture in a 1.05% Al containing TRIP steel [28]. The composition of the TRIP steel was 0.15% C, 2.45% Mn, 0.025% Nb, 0.005% S, 0.0065% N.

The hot ductility of high Al, TWIP steels is found, as might be expected, to be dependent on the product of [Al][N], decreasing as the product increases (Figure 13), inferring that the higher the product the more AlN is precipitated at the boundaries.

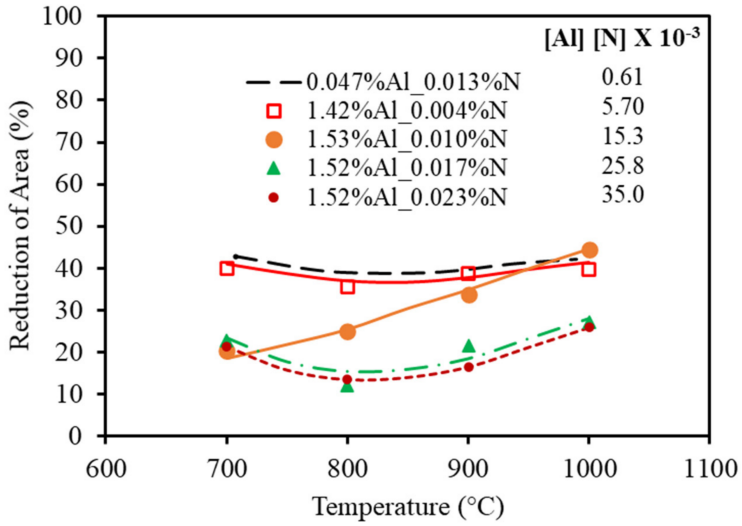

Figure 13. Hot ductility curves for TWIP steels having different products of [Al][N], from 0.61 to 35×10^{-3}. Al additions varied from 0.047 to 1.5% and N from 0.004 to 0.0023%. The base composition of the steels was 0.6% C, 18% Mn and 0.006% S [30,31].

The high Al, as well as the high Mn content of these TWIP steels, prevents DRX from occurring and encourages grain boundary sliding [32] so that the ductility of unrecrystallised austenite, which is the ductility relevant to the straightening operation, is poor and actually decreases with the increase in test temperature, Figures 14–16. The curves in Figure 14 illustrate very well the difference when and when not TWIP steels show DRX. When there is no Al present, top curve in Figure 14, DRX can take place giving much better ductility but this is not relevant to the straightening operation. In contrast, for the high Al containing TWIP steels—the lower curves in Figure 14—DRX is difficult and often does not occur in the straightening temperature range, as shown in Figure 14. The overall ductility given by the hot tensile test can then be used to assess cracking susceptibility for the straightening operation. It can be seen that the ductility is now poor below the 35–40% RA, often quoted to avoid cracking, Figures 14–16.

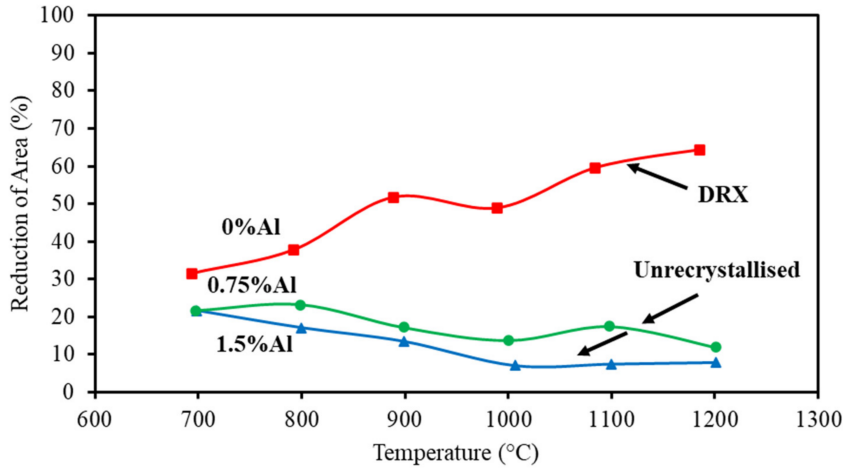

Figure 14. The hot ductility of TWIP steel at different Al content for the base composition: 0.6% C, 0.008% S, 18% Mn and 0.01% N [32]. The top curve is for a TWIP steel free of Al and shows the big improvement in overall ductility when DRX occurs.

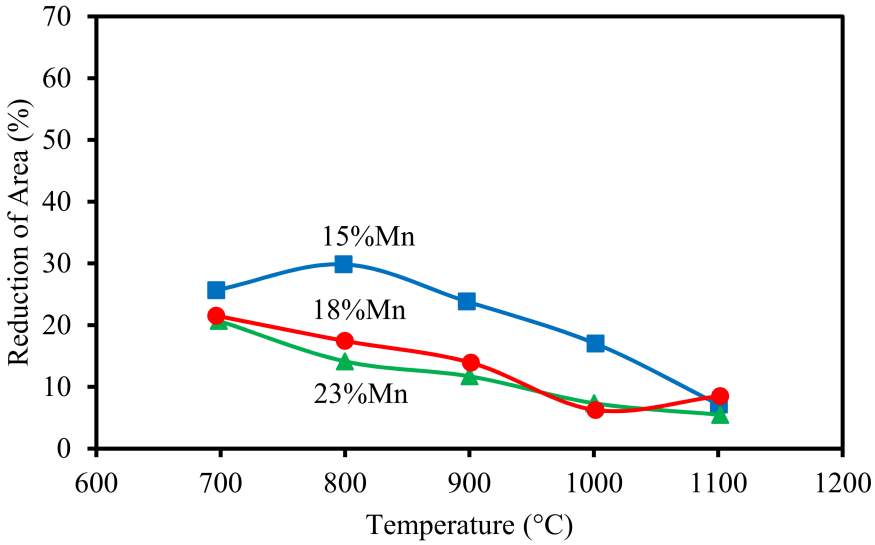

Figure 15. Influence of Mn content on the ductility of high Al containing TWIP steels. The base composition of the steels was 0.6% C, 0.007% P, 0.008% S and 1.5% Al [32].

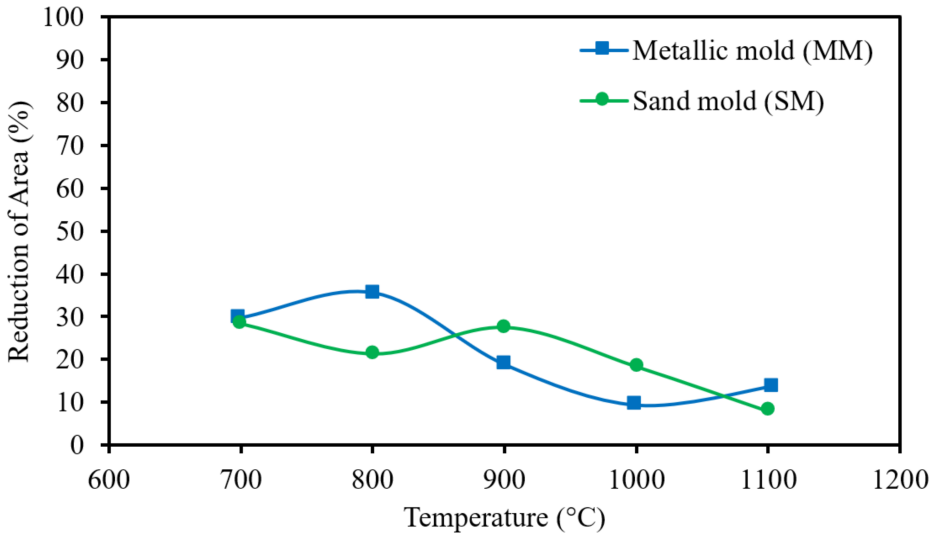

Figure 16. Hot ductility curves for a TWIP steel having the composition 0.45% C, 22% Mn, 1.5% Al and 1.5% Si with 0.02% Ti for two different cooling rates, the tensile specimens were cast in metallic and sand molds [33].

Attention has therefore been given to finding ways which will mitigate this effect of a high Al addition and prevent cracking during straightening. The present most satisfactory approach has been to use a B addition with these high Al containing steels [22,27,34–40]. B has been found to segregate to the boundaries in both TRIP and TWIP steels and when there in solution, it strengthens the austenite grain boundary even when the thin film of AlN is present. In order to achieve this, the B needs to be protected from forming BN by having a stronger nitride former present. If BN forms in the matrix and at the boundaries, ductility is often impaired [40–42]. By using Ti, TiN is formed instead of BN. The amount of Ti generally added is in excess of the stoichiometric composition for TiN, so as to ensure that there is no N left in solution which might form BN. Provided the average cooling rate after melting is sufficiently slow (~15 °C/min), which is close to that of the secondary cooling when thick slab casting, the TiN will be sufficiently coarse to have little influence on the hot ductility [43,44]. There are many explanations accounting for B segregation to the boundaries improving hot ductility [22,27,34–40] and as it is non-equilibrium [45,46], the cooling rate is very important and significant segregation only occurs in the range

10–100 K/min [19]. Moreover, if sufficient Ti is added to combine with all the N only a small amount of B, 0.003% needs to be added, this being the maximum solubility of B in ferrite at a temperature even as high as 900 °C [47].

However, a word of warning: it should be noted that according to thermodynamic analysis, under equilibrium conditions, AlN can still form at the boundaries even when high Ti levels are present and the Ti/N ratio is well above the stoichiometric for TiN formation, e.g., in Figure 17 for a steel with a Ti:N ratio of 7. This is because of all the "microalloying" additions in this high Al, TWIP steel, AlN is the first to precipitate out on solidification under equilibrium conditions (1440 °C in Figure 17) and although it can go back into solution when TiN starts to form (1400 °C), it can re-precipitate out again at lower temperatures, 1100 °C in Figure 17. Whether this occurs under the non-equilibrium conditions existing on continuous casting is not clear, particularly as AlN is so sluggish in precipitating out [29] and more studies are required to establish the conditions in which AlN is formed under the non-equilibrium conditions applying in Industry.

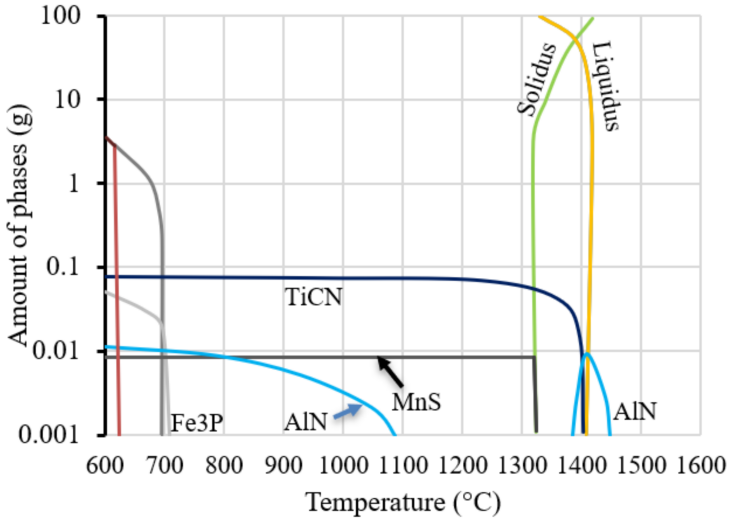

Figure 17. Thermo-Calc precipitation predictions for a TWIP steel with a composition of 0.61% C, 18.0% Mn, 0.003% S, 0.062% Ti, 1.54% Al and 0.007% N. Ti:N ratio of 7:1.

The S level has also been shown to be very important for attaining good hot ductility since AlN precipitates much more readily when MnS inclusions are present as they act as nuclei for the AlN to precipitate out on, Figure 18a,b.

Steenken et al. [48] have also shown that in high Mn steels, when the Al level is less than 3%, MnS forms first at higher temperatures and probably act as nuclei by decreasing the interfacial energy needed for AlN precipitation. They also suggest that when the Al > 3%, AlN forms first at high temperatures and likely acts in its turn as a nucleus for MnS precipitation. A low S level is therefore a necessary requirement for good ductility in these steels. However, it is not a panacea as can be seen from Figure 11b, in which the TWIP steel had a very low S level (0.002%) yet still gave rise to a thin coating of AlN at the grain boundaries. Hence, removing MnS, i.e., reducing the S level, will make it more difficult for AlN to precipitate out at the boundaries, reducing the amount of AlN that is precipitated there, but this will not eliminate it.

This influence of MnS on hot ductility was shown by Kang et al. [49], who examined the influence of three S levels, 0.003, 0.010 and 0.023% S on the hot ductility of high Al containing TWIP steels and found that only at the lowest S level (0.003%) was ductility notably better, Figure 19. Up to the temperature of 900 °C, Figure 19, the hot ductility curves were similar but at higher test temperatures the hot ductility for the very low S-bearing steel (0.003% S), significantly improved, the RA value being 35% higher than that for the higher S steels. Kang et al. [49] showed that independent of the S level, the AlN precipitated out as a coarse precipitate, but where it precipitated, it depended on the S level. When the

S levels were >0.01%, the AlN precipitated out in the form of very coarse dendritic rods at the dendritic and austenite grain boundaries, promoting intergranular fracture, Figure 18a. At the lower S level, precipitation of AlN was more difficult and was mainly associated with MnS inclusions that were situated in the matrix, Figure 18b [49].

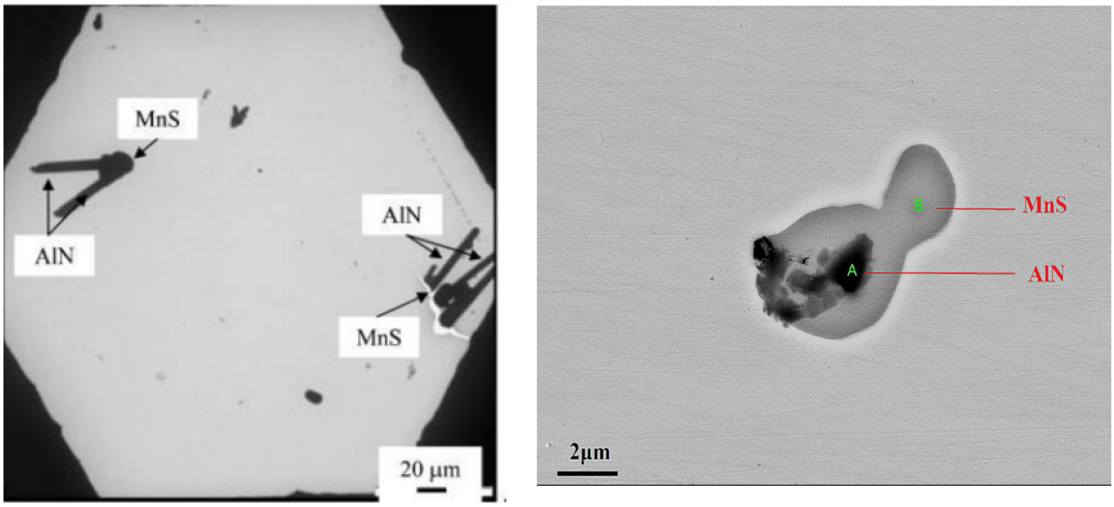

(**a**) (**b**)

Figure 18. (**a**) MnS inclusions acting as a nucleus for AlN precipitation in TWIP steels having S in the range 0.01–0.023% and (**b**) a similar steel with a low S, content of 0.003% [49].

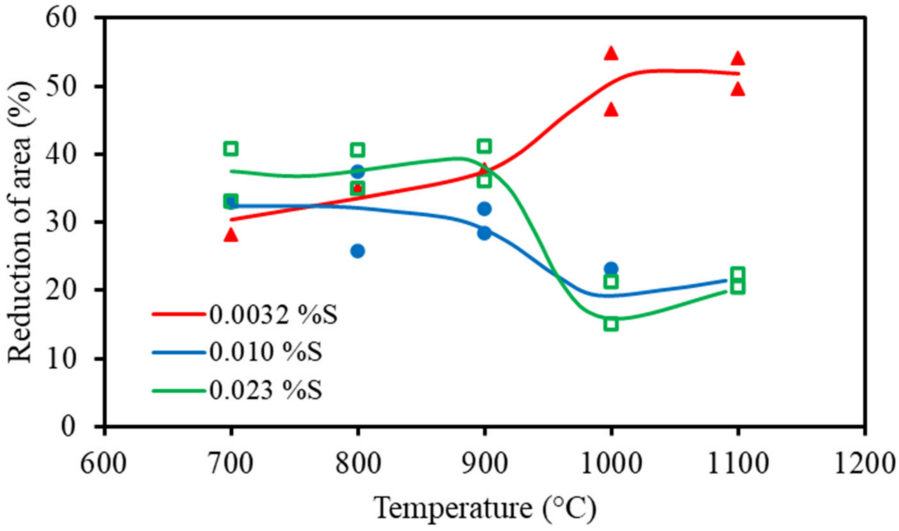

Figure 19. Hot ductility curves for three TWIP steels having 0.003, 0.01 and 0.023% S with base composition: 0.6% C, 18.3% Mn, 1.5% Al and 0.009% N [49].

The MnS inclusions also offer themselves as very suitable sites for B to segregate to and when present, rather than segregating to the boundaries, where it is required, it segregates to the MnS inclusions [50]. Ideally, complete removal of S is desired but industrially, the limit is normally set at ≤0.01%.

5. Influence of P

P like Al and Si can be used in TRIP steels as it is a ferrite former to delay the precipitation of C in ferritic bainite and hence increase the C in the austenite. In order to activate the "TRIP effect", so that ~10% stable retained austenite can be formed at room

temperature, Chen et al. have shown that ~0.1% P is required, with a minimum of 0.5% Si [51].

Previous work [18] has shown that P segregation to the boundaries can improve or worsen the hot ductility of low C steels (<0.25% C) depending on the degree of segregation. Even at low levels, 0.016% of P [52] if it segregates sufficiently to form the low melting point iron phosphide phase ductility is impaired. If this is prevented, improvements in ductility can be obtained, as shown in Figure 20, for a variety of reasons: (1) P segregating to the thin band of ferrite and strengthening it by interstitial hardening [53], (2) preventing the more deleterious precipitates from forming by preferentially taking up the vacant sites which they need for precipitating out on [54,55] and (3) preventing GBS by absorbing the vacant sites needed for cracks to propagate [53]. It would be expected that the same behaviour as shown for HSLA steels would apply to TRIP steels. As a high addition, ~0.1% P is required to delay carbide precipitation when used to form a TRIP steel, control of segregation will always be very important.

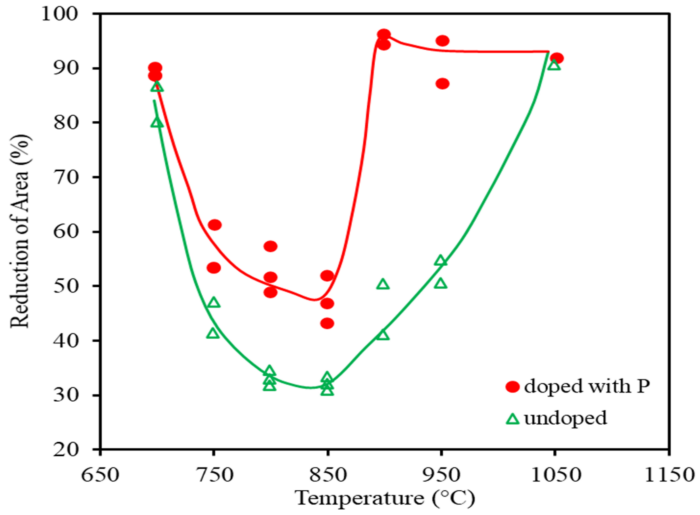

Figure 20. P addition of 0.054% P improving the hot ductility of a low alloy Cr-Mo steel [53].

In high C steels this low melting point phase forms easily and ductility can dramatically decrease in the temperature range 950–1050 °C, Figure 21a, <10% RA, even for low P (0.007% P) plain C-Mn steels [56].

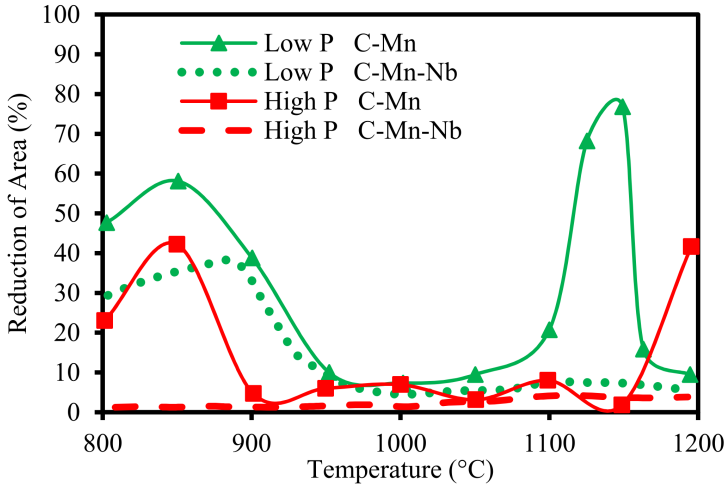

(**a**)

Figure 21. *Cont.*

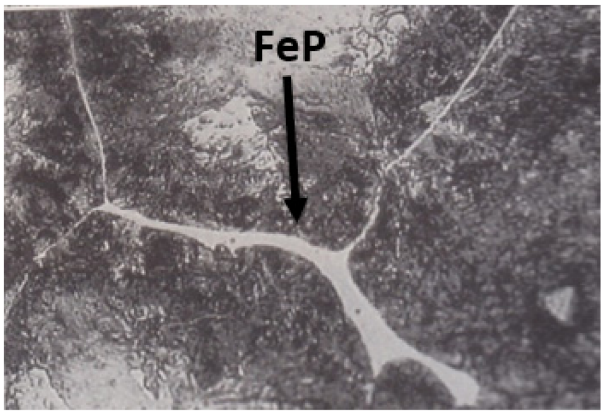

(**b**)

Figure 21. Influence of P on the hot ductility of high C (0.6%), low alloy steels: (**a**) hot ductility curves for as-cast C-Mn-Nb-Al and plain C-Mn steels at two levels of P, 0.007% and 0.045% (**b**) low melting point iron phosphide phase at prior austenite grain boundaries in the low P plain C-Mn steel. The base composition of the steels was 0.6% C, 2% Si, 0.8% Mn and 0.025% Al with and without 0.03% Nb [56].

This difference between high and low C steels arises because for steels in the higher C range ≥0.25%, the melt solidifies as the closed packed austenite phase and not the more open bcc delta ferrite. As a result, the last liquid to solidify will have more P in solution when it solidifies as austenite than when it solidifies at lower C contents in the delta ferrite [57]. Yashima et al. [58] calculated that for a steel with 0.25% C and 0.04% P, the last liquid to solidify as austenite will contain as much as 5% P. In contrast, a steel with 0.1% C with the same P level would have when solidifying in delta ferrite, 1% P present in the final interdendritic liquid.

Similar behaviour to that shown in Figure 21 is noted in the high C TWIP steels, Figure 22, the ductility decreasing with increase in P level [56]. Even increasing the P level from 0.007%, curve 1, to 0.019%, curve 2, causes the ductility to deteriorate and the iron phosphide films are present in the lowest P containing steel but less extensively. Hence, P levels should be as low as possible in these high C, TWIP steels (<0.01% P) as it performs no useful function as it does in TRIP steels, delaying carbide precipitation.

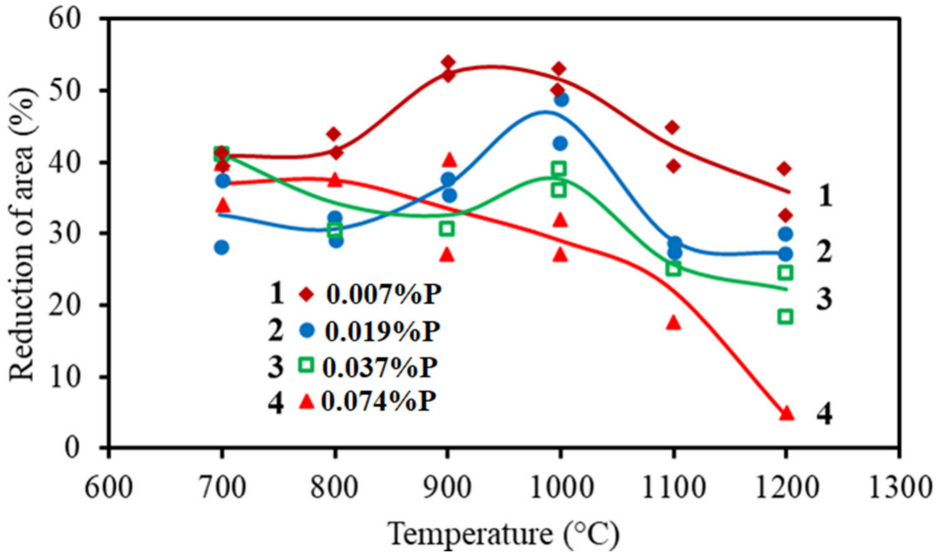

Figure 22. Influence of P on hot ductility curves of a TWIP steel. Steels had a base composition of 0.6% C, 0.3% Si, 18.2% Mn, 0.005% S, 1.5% Al, 0.01% Ti, 0.007% N with a B addition of 0.0026% B and P additions of 0.007, 0.019, 0.037 and 0.074%, steels, 1–4, respectively [59].

6. Influence of Si

There is little data in the literature on the hot ductility of high Si-containing steels. In contrast to Al and P, Si appears to have little influence on the depth of the trough in low C steels but because it raises the Ae3 and Ae1 (the lowest temperature at which austenite can form on heating. It represents transformation under equilibrium conditions), it moves the hot ductility curves to higher temperatures, Figures 23 and 24 [60,61].

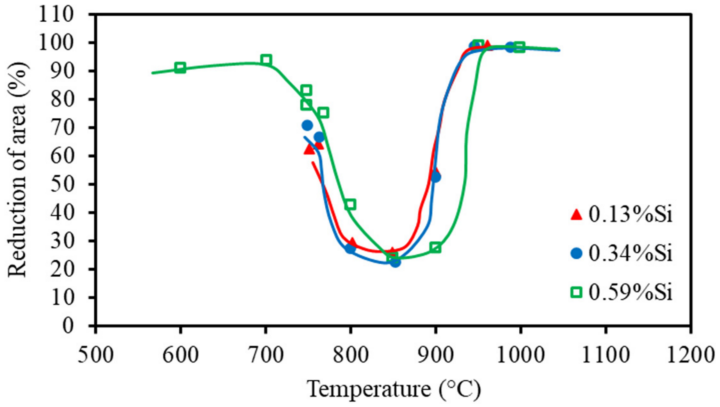

Figure 23. Influence of Si on the hot ductility curves of plain 0.1% C, 1.2% Mn steels (Al free) having 0.011% N. Curves move to higher temperatures with increasing Si level [60].

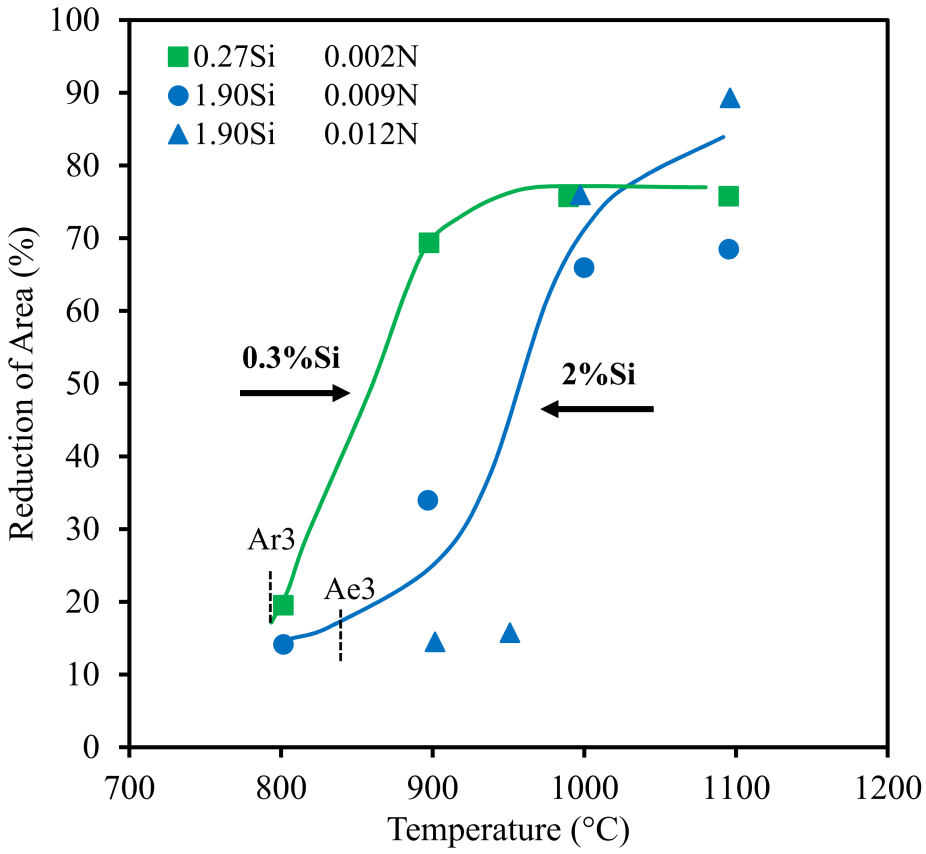

Figure 24. Influence of Si on the hot ductility of medium C steels (0.5% C, 0.01% N), again curve moves to higher temperature with increase in Si content [61].

This means that, if the bending temperature for steels, including TRIP, is based on the steel being fully austenitic, i.e., just above the Ae3, so as to avoid the film of ferrite present in the trough, the temperature chosen for the straightening temperature for high

Si containing steels should be increased appropriately. Examination of Figures 23 and 24 suggests that an addition of 1% Si would involve increasing the bending temperature by ~60 °C.

For TWIP steels as there is no ductility trough, Si additions should have little influence on the ductility.

7. Influence of Precipitation on Increasing the Room Temperature Yield Strength of TWIP Steels in Relation to Their Hot Ductility

Although the work hardening capacity is very high for TWIP steels, resulting in very high tensile strengths, the actual room temperature yield point can be low compared to other AHSS (advanced high strength steels) and this has limited their use [1].

Attention therefore has been directed towards increasing the yield strength by adding the microalloying elements, Nb, V and Ti to give precipitation hardening and grain refinement [62–64].

The work of Scott et al., Figure 25 and Table 2 [62] shows that for cold worked and annealed strip, of the micro-alloying additions Ti, Nb and V, Ti gives the highest hardening for additions up to 0.1% but above this amount there is little further change. This is in contrast to V, which increases the room temperature yield strength in a linear manner and above 0.3% exceeds the yield strength of Ti containing steels, Figure 25 [62]. This figure, Figure 25, does not separate the contribution to the increased yield strength from grain size and precipitation hardening, but shows from a design perspective, V rather than Ti, is the best addition for consistently increasing the strength. Nb in contrast seems to have only a small influence on increasing the room temperature yield strength, although further work is needed to confirm this (bottom curve in Figure 25).

Hence, to give a worthwhile increase in the yield strength of 100 MPa, one would, according to the work of Scott et al., need ~0.2% V, 0.55% Nb or 0.075% Ti [62].

Other research investigators [63,64] concentrating on V alone in these TWIP steels found similar room temperature strengthening by V in a cold rolled and annealed strip [63] and a smaller but nevertheless substantial increase in hot rolled and annealed strip [64].

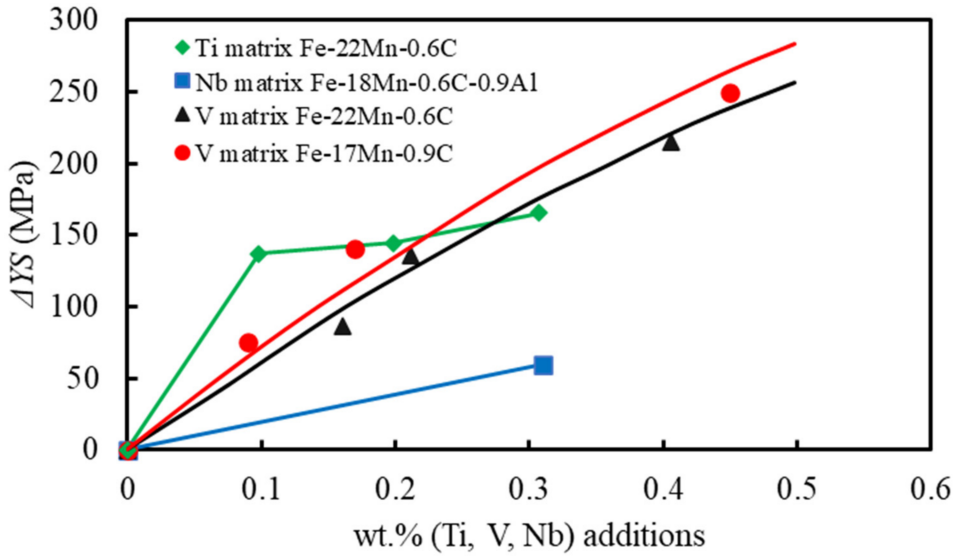

Figure 25. A comparison of the room temperature yield strength increases in TWIP steels for cold rolled and annealed strips as a function of the microalloying additions, Ti, Nb and V [62].

Table 2. Strengthening coefficients (MPa/wt.%) of various elements after cold rolling and annealing TWIP steels [62].

Element	Strengthening Coefficient of Microalloying Additions below 0.1 wt.%
Ti $\leq$ 0.1	1380 MPa/wt.%
Nb	187 MPa/wt.%
V (up to 0.4%)	>530 MPa/wt.%

8. Hot Ductility of V Containing High Al, TWIP Steels

Because of the interest in adding V for strengthening the room temperature yield strength, Kang et al. [22] have examined the influence of V additions on the hot ductility of high Al, TWIP steels, Figure 26 and found that ductility was generally below that required to avoid cracking on straightening. The base composition of the steel in Figure 26 was 0.6% C, 18% Mn, 1.5% Al, 0.001% S, 0.0014% P with V additions of 0.05, 0.11, 0.29, 0.5 and 0.75% V, steels 1–5, respectively. An average cooling rate of 60 °C/min and strain rate of 3 × 10^{-3} s^{-1} was used to represent thick slab casting conditions. The lower V containing steels, steel 1 (0.05% V) and 2 (0.1% V) in Figure 26 were found not to show any precipitation in the straightening temperature range 700–1000 °C but ductility was still poor for test temperatures above 850 °C, being <35–40%, the criterion used to avoid cracking [22]. Thermo-Calc analysis showed that VC would precipitate out on cooling but at temperatures below the straightening temperature range and so would not influence cracking susceptibility [22]. At the 0.29% V level, steel 3, fine dynamic precipitation of VC occurs, Figure 27 making the ductility even worse and at the 0.5%V level with more precipitation of VC, steel 4, the RA value was <30% RA throughout the whole of the straightening temperature range, Figure 26.

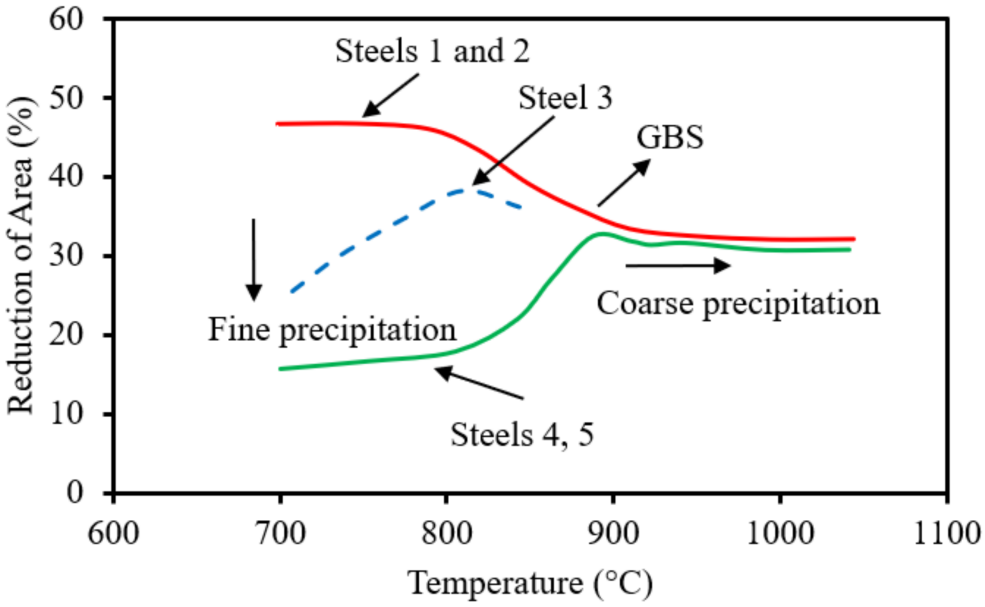

Figure 26. Hot ductility curves for V containing high Al TWIP steels 1–5 having respectively, 0.05, 0.11, 0.29, 0.5 and 0.75% V [22].

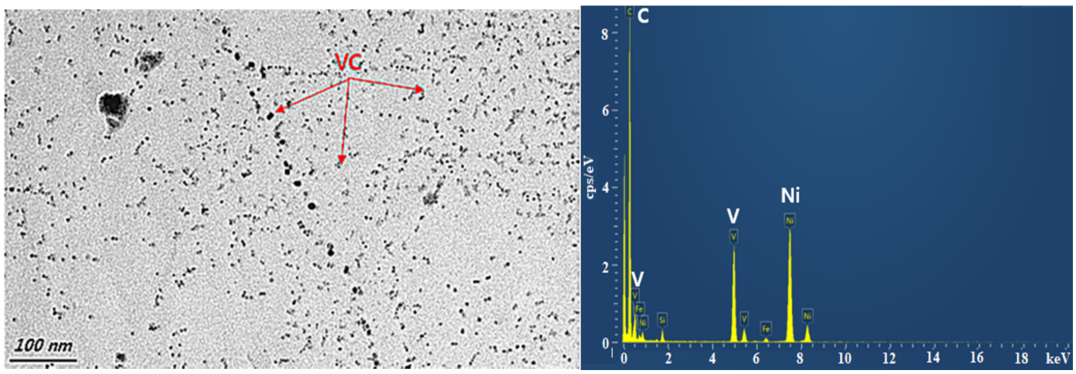

Figure 27. Fine VC precipitation in a 0.3% V containing TWIP steel both at the grain boundaries and within the matrix [22]. A Ni grid was used to support the replica.

Examination of the hot ductility curves for steels 3–5 (~0.3–0.7% V) in Figure 26, suggests V at the levels required to attain a meaningful increase in the room temperature yield strength, (≥100 MPa), i.e., ~0.2% V would result in poor ductility.

To see whether a B addition would improve ductility, Kang et al. added 0.003% B to the V containing TWIP steel having 0.5% V, curve 4 in Figure 26. As is usual, enough Ti was added to combine with all the N (0.06% Ti, 0.01% N) and so protects the B and allows it to segregate to the boundaries, Figure 28 [22]. The ductility was found to improve by 10% in RA over the whole temperature range in which the straightening operation takes place, Figure 28. This high V addition (0.5%) would probably be good for enhancing the room temperature yield strength but the ductility for the lower straightening operational temperature range <900 °C would be poor even with a B addition, Figure 26 and likely to cause cracking on straightening. Thus, from this work, once VC starts precipitating out, at the 0.3% V level, as shown in Figure 27, the ductility deteriorates too much to ensure cracking will not occur. However, it is possible a lower V addition, ~0.2% to high Al, Ti-B treated TWIP steel may increase the room temperature yield strength by ~100 MPa, as well as just meeting the requirement for avoiding cracking when straightening, but further work would be needed to confirm this.

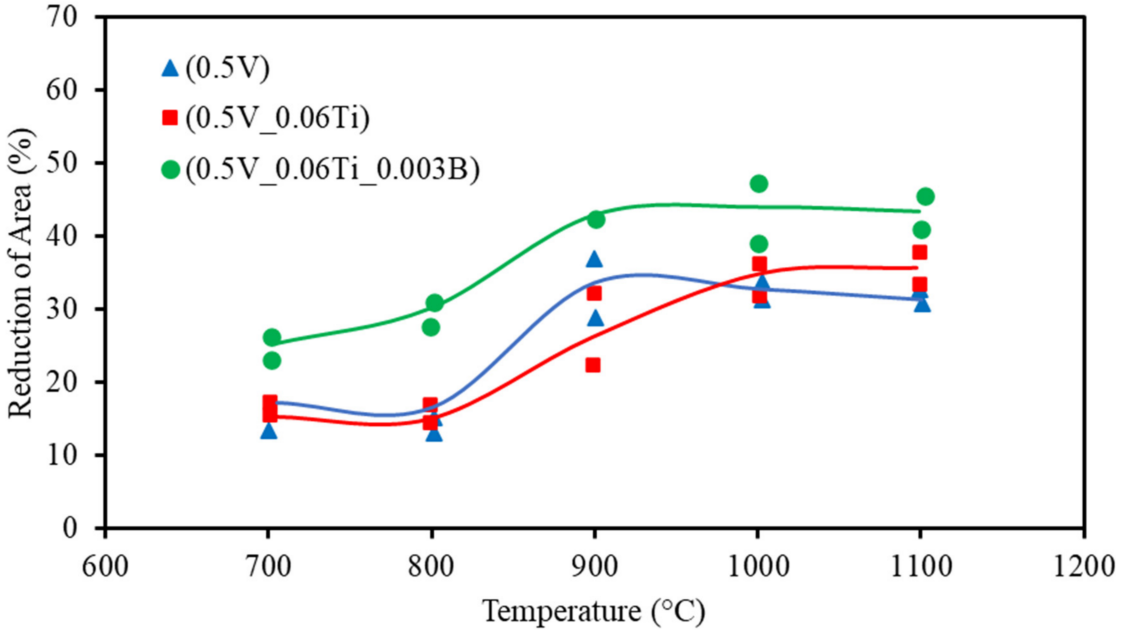

Figure 28. The beneficial influence of B on the hot ductility of a high V (0.5% V), TWIP steel [22].

Again, the differences in hot ductility behaviour between TWIP steels showing DRX and TWIP steels in their un-recrystallised state is highlighted by comparing the hot ductility curve of Kang et al. [22] with the curve established by Salas-Reyes et al. [33] for a TWIP steel with the same V addition of 0.1%, Figure 29.

Salas-Reyes et al. [33] found that ductility was low at the low and high temperature ends of the straightening temperature range, 700–1000 °C, but there was an intermediate range when ductility was good, 80% RA, Figure 29 (a) (top curve). This they explained in terms of the competing processes of GBS, recovery and DRX on influencing the ductility. At the low temperature end, 700 °C, there is no DRX and GBS is the dominating process controlling the ductility. At higher temperatures 800–900 °C, DRX occurs and dominates the ductility realising high RA values. At the high temperature end, DRX will still probably be taking place but GBS is now the dominating process and before DRX can exert its beneficial effect, failure occurs and as a result ductility is poor. However, this is very different to the behaviour noted by Kang et al. [22], in which the composition of the TWIP steel did not allow DRX to take place, so the competing processes influencing the ductility are only recovery and GBS, and as the latter dominated, ductility was always poor and became worse as the test temperature increases, Figure 29 (b) (lower curve). Whereas, Salas-Reyes work [33] is very relevant to the hot ductility required for hot forming, Kang et al. work [22] is relevant to the straightening operation where DRX is not possible. It can be seen from Figure 29 (b), that when the austenite is un-recrystallised, as it is when straightening, the RA value is <40% for most of the straightening temperature range and cracking is likely.

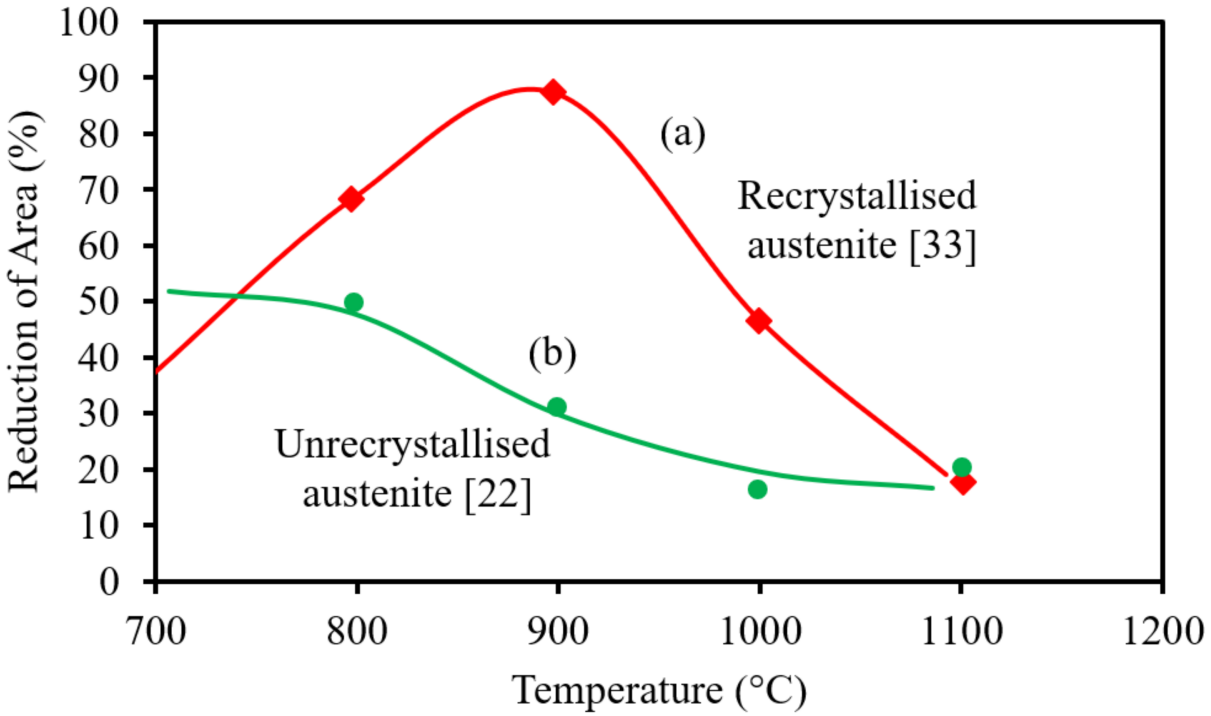

Figure 29. Hot ductility curves for high Al TWIP steels with the same V content, 0.011% V, (a) recrystallised austenite (b) un-recrystallised austenite. Compositions of TWIP steels were: Recrystallised top curve –21% Mn, 0.56% C, 1.3% Si, 1.50% Al, 0.011% V and 0.012% N [33]. Unrecrystallised bottom curve –18% Mn, 0.61% C, 0.2% Si, 1.54% Al, 0.011% V and 0.007% N [22].

9. The Beneficial Influence of a Ti-B Addition on the Hot Ductility of High Al, TWIP Steels

In the pursuit of a composition which will avoid cracking in these high Al steels, Kang et al. [22,26,27,30,65] and Qaban et al. [66] have examined the hot ductility of a series of 0.6% C, 18% Mn, 1.5% Al TWIP steels having a variety of micro-alloying additions, B, Ti, Nb, V and various combinations of Nb-V, Nb-Ti-V, V-B, V-Ti-B, Ti-B. The cooling rate

chosen was 60 K/min with a strain rate of 3×10^{-3} s^{-1}. A selection of these hot ductility curves is given in Figure 30 and their compositions are given in Table 3. Moreover, given in Table 3 is the RA value for the test temperature of 900 °C.

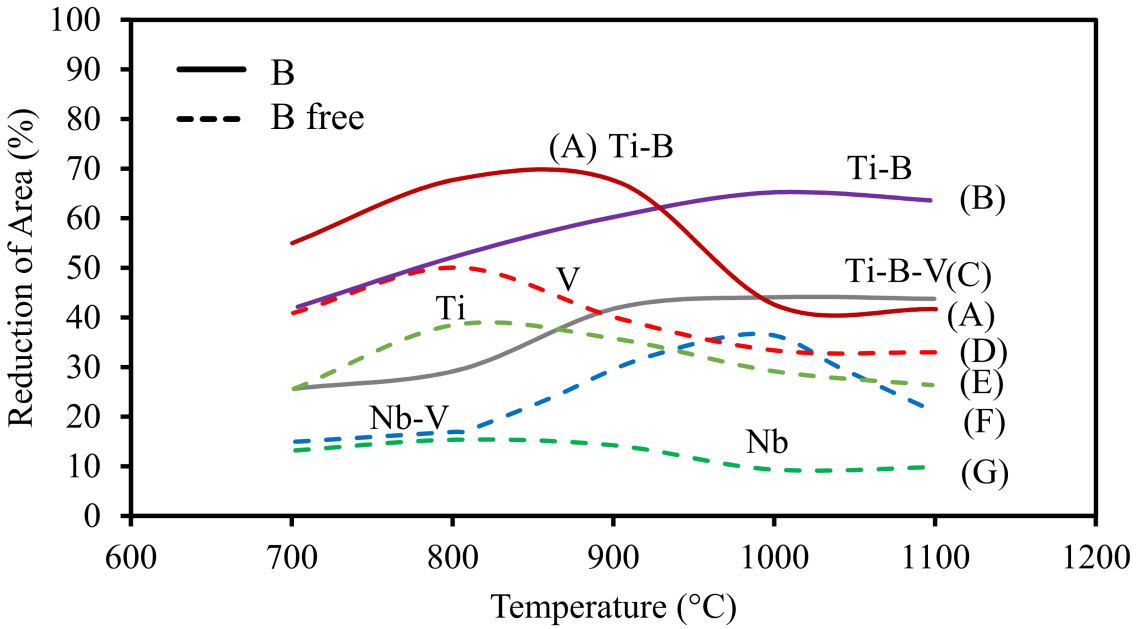

Figure 30. Hot ductility curves for high Al TWIP steels having a variety of microalloying elements, Nb, Nb-V, Ti, V, Ti-B and Ti-B-V. Steels had the base composition 0.6% C, 18% Mn, 1.5% Al and the cooling rate and strain rate were 60 K/min and 3×10^{-3} s^{-1}, respectively [22,26,27,65,66].

Table 3. Composition of steels in Figure 30, with their % wt.per.cent and %RA at 900 °C.

No	Steel	C	Mn	S	Al	Nb	Ti	V	N	B	%RA 900 °C	Ref.
(A)	Low Ti-B	0.60	18.0	0.003	1.48	-	0.041	-	0.009	0.0026	68	[27]
(B)	High Ti-B	0.55	17.6	0.004	1.44	-	0.098	-	0.009	0.0017	61	[27]
(C)	Ti-B-V	0.61	18.0	0.001	1.54	-	0.062	0.50	0.012	0.0026	42	[22]
(D)	V	0.61	18.0	0.001	1.52	-	-	0.052	0.006	-	39	[22]
(E)	Ti	0.62	17.9	0.004	1.53	-	0.041	-	0.009	-	37	[27]
(F)	Nb-V	0.61	18.3	0.005	1.55	0.03	-	.11	0.006	-	30	[65]
(G)	Nb	0.55	18.3	0.002	1.2	0.02	-	-	0.006	-	14	[65]

Ductility can be seen to vary substantially in Figure 30 from 10–15% (curve G, 0.02% Nb and low N) to 40–70% (curve A, Ti-B) for the straightening temperature range, 700–1000 °C. For the B free steels, D, E, F and G, Figure 30 and Table 3, a V addition of ~0.05% (curve D) was found to give the best ductility. However, even this small addition of 0.05% V, curve D, gave RA values of <40% at temperatures ≥900 °C [22], Table 3. An addition of B, (curves A, B and C), significantly improved the ductility of these microalloyed TWIP steels. Of these B treated TWIP steels, protected by Ti, curves A and B gave the best ductility and Mintz et al. [21] have suggested this alloying combination with its likely, higher room temperature yield strength (0.05 to 0.1% Ti), may, presently be the best choice [27].

Salas-Reyes et al. [33], as already discussed, have similarly examined the influence of Ti and V additions on the hot ductility of these TWIP steels and Meija et al. have extended the range of their microalloying additions to Ti, B [34] and Nb, Mo [67]. The main difference between these investigations and those of Kang et al. [22,26,27,30,65] and Qaban et al. [66]

is in the compositions of the TWIP steels, in having different Mn and C contents as well as the presence or absence of Si. This will influence the SFE and the ease of DRX and hence the hot ductility performance.

10. Relationship of Overall Hot Ductility to the Hot Ductility Needed for the Straightening Operation

Mintz and Qaban [21] have proposed a model which can give some indication of the cracking susceptibility based on Salas-Reyes et al. [33] and Meija et al. observations [67] and can explain the difference in hot ductility behaviour shown by these high Mn TWIP steels, Figure 29 (a) and (b). When there is no evidence for DRX in the straightening temperature range, 700–1000 °C, GBS dominates over recovery processes and the ductility decreases with increasing temperature as shown in Figure 29, curve (b) and in the model Figure 31a.

However, Salas –Reyes et al. [33] and Meija et al. [34,67] found in their steels that GBS often dominated at the low and high temperature ends of the straightening temperature range, 700–1000 °C but there was an intermediate range when DRX occurred leading to another type of curve Figure 29, curve (a) and Figure 31b in the model.

Mintz and Qaban [21] have suggested that the best way to treat these hot ductility curves for assessing cracking susceptibility is to assume that one can approximate the relationship of grain boundary sliding with temperature as a linear relationship and draw a line (solid line in Figure 31c) joining up the two regions of grain boundary sliding and use this solid line to give an approximate measure of the hot ductility for the un-recrystallised austenite.

On this basis in the model, if for example the RA value was 40% at 700 °C and 20% at 1000 °C, Figure 31c, then the value of RA for the un-recrystallised state is likely to be lower than 40% in the temperature range 800–1000 °C and importantly cracking may occur even though, when DRX takes place the RA value may be as high as 80%, Figure 29 (a).

Although the model seems to be useful for giving some indication of the cracking susceptibility on straightening there is evidence from the hot ductility curves, Figure 30 that in the lower temperature range, 700–800 °C recovery keeps pace or slightly outstrips GBS even though the general effect on increasing the test temperature is for GBS to be dominant. Moreover, when fine dynamic precipitation is present in the lower temperature range <900 °C ductility decreases so much in Figure 27 that ductility is better at the higher temperature even though GBS is outstripping recovery, Figures 26 and 28.

There is an obvious need to put this model on a more rigorous mathematical basis, relating the RA value to the degree of GBS and recovery that occurs with the increase in test temperature, but presently this is the best alternative.

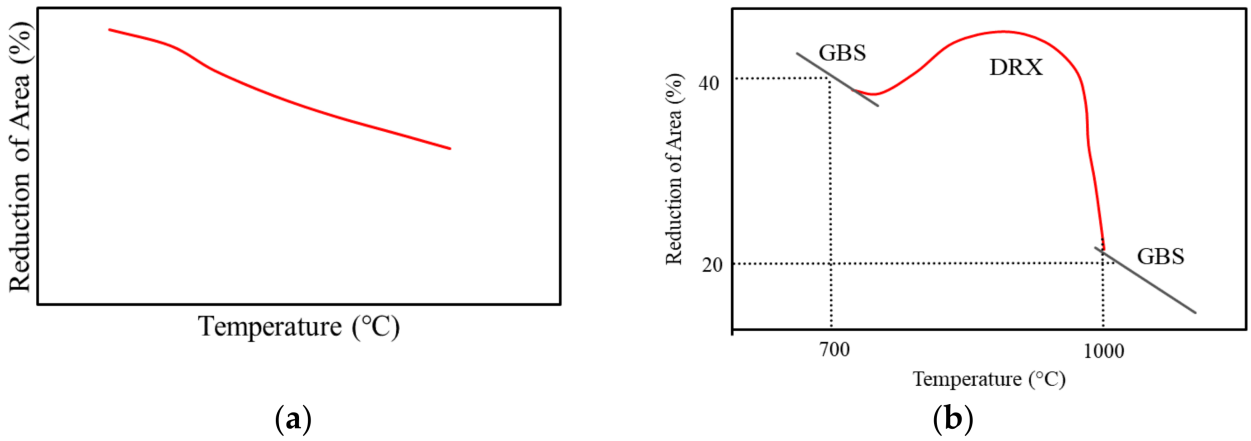

Figure 31. *Cont.*

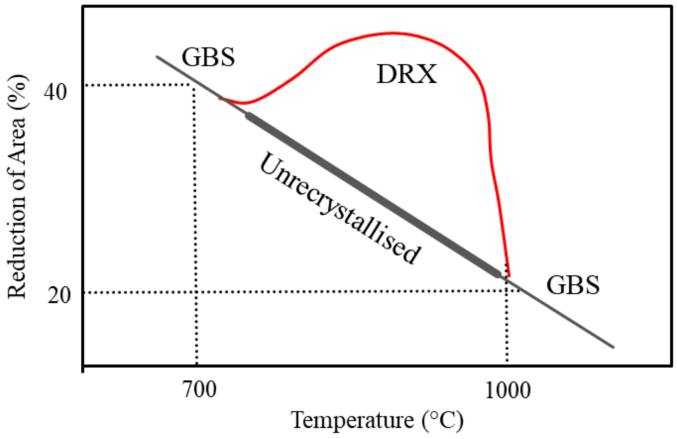

(**c**)

Figure 31. Schematic types of hot ductility curves for high Mn TWIP steels (**a**) No DRX, no fine matrix precipitation, the curve is relevant to straightening (**b**) GBS at the low and high temperature ends of the straightening temperature range but DRX in intermediate temperature range, curve relevant to hot forming (**c**) Separation of curve in (**b**) into regions of GBS and DRX and drawing a straight line relationship for continued GBS in the temperature range in which DRX is occurring [21].

Hence, as it is the ductility of the un-recrystallised austenite that is important for assessing cracking susceptibility, it is not surprising that these TWIP steels are difficult to continuous cast without cracks forming.

11. Influence of Nb on Hot Ductility of TWIP Steels and Importance of Having a High N Content to Give Good Ductility

Although Nb does not appear a good microalloying element to add for strengthening the room temperature yield strength compared to V, Qaban et al. [62] have also explored the ductility of Nb containing TWIP steels and this has revealed some important findings with regards to improving the ductility generally in these steels, Figure 32. A series of Nb (0.032% Nb) and Nb free, B containing TWIP steels were examined with Ti additions varying from 0.019 to 0.1% and N contents from 0.007 to 0.011%, Table 4. What is very clear from the curves in Figure 32, is that at a high level of N, ~0.1%, curves 1, 2 and 3, ductility is very good in the Nb-containing steels, and remains high as the Ti level increases. Even when the Ti level is as high as 0.075%, ductility is good, curve 1.

Without Nb, when only Ti is there and the N level is low, steel 6 in Table 4 and curve 6 in Figure 32, the ductility is poor, even with a B addition but improves when the N level is increased to 0.009%, curve 4, achieving RA values > 40% throughout the temperature range 700–1100 °C, Figure 32 [66]. Qaban et al. [66] have suggested that a high [Ti][N] in the Nb free steels, 4, 5 and 6 in Table 4 will cause the TiN precipitation to occur at higher temperatures and so will be coarser and give improved ductility, curves 4, 5 and 6 in Figure 32. Surprisingly, a 0.03% Nb addition improved the ductility even more, the RA values being >55% through-out this temperature range, curves 1, 2 and 3, Figure 32 [66].

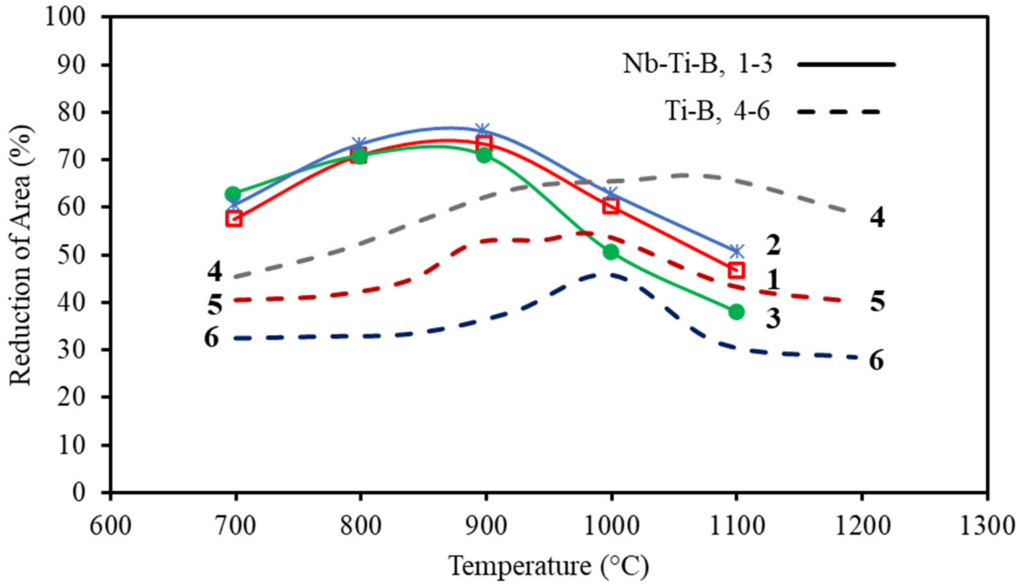

Figure 32. Influence of Nb on the hot ductility of high Al, Ti-B containing TWIP steels. The composition of the steels (1–6) is given in Table 4. Cooling rate and strain rate were 60 K/min and 3×10^{-3} s^{-1}, respectively [66].

Table 4. Compositions wt.per.cent of steels in Figure 32 together with the Product of [Ti][N] and RA value at 900 °C [66].

Steel	Nb	Ti	B	N	[Ti][N] $\times 10^{-4}$	RA% 900 °C
1	0.033	0.075	0.0028	0.011	8.25	72
2	0.032	0.030	0.0028	0.010	3.00	76
3	0.031	0.019	0.0027	0.009	1.71	70
4	-	0.098	0.0017	0.009	8.82	62
5	-	0.105	0.0026	0.0073	7.67	53
6	-	0.100	0.0027	0.0068	6.8	35

Turkdogan [68] previously has suggested in HSLA steels, that the coarse TiN particles formed after solidification act as nucleation sites for Nb(CN) precipitation and therefore encourage the Nb to precipitate at high temperature leaving less available to precipitate dynamically on deformation, in the very fine form that is so detrimental to hot ductility [19]. From this aspect there seems to be a very positive use in having the Ti as a microalloying addition and having high N in the steel so that the [Ti][N] product is high, Table 4, encouraging precipitation of Ti(CN) at high temperature so that they are coarse and subsequently serve as a suitable nucleation site for the precipitation of Nb(CN).

Precipitation of Nb(CN) on the TiN particles is favoured because TiN and Nb(CN) are mutually soluble [69] and so the Nb(CN) can precipitate out on the TiN and provided the TiN is coarse as in Figures 33 and 34 this will result in even coarser particles and better ductility. Unfortunately, as already mentioned, Nb has been found to give a low strengthening coefficient in these steels, Table 2, but further work is needed to confirm this observation and there is still the possibility that a Nb, Ti-B combination may give a higher room temperature yield strength as well as being cast satisfactorily.

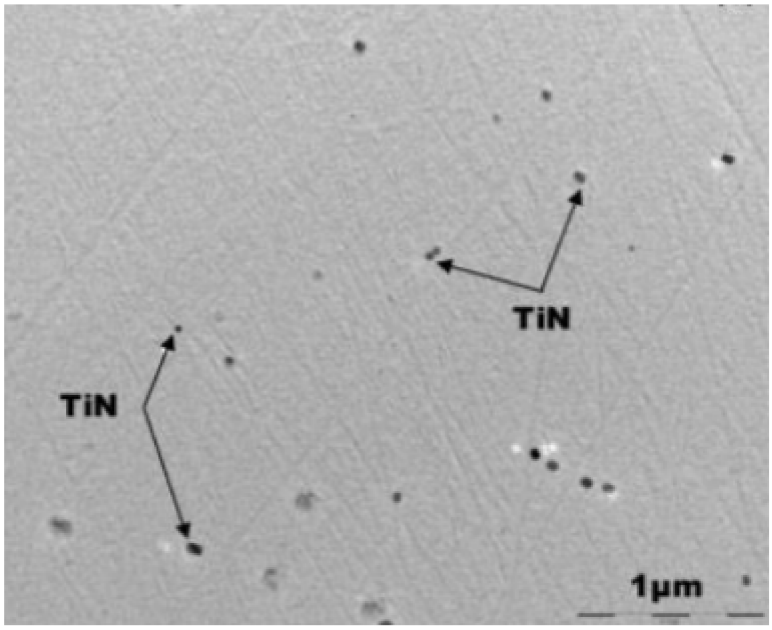

Figure 33. Coarse TiN precipitates in 0.1% Ti, containing B steel, TWIP steel free of Nb, tested at a 1000 °C, Steel 4 in Table 4 [27].

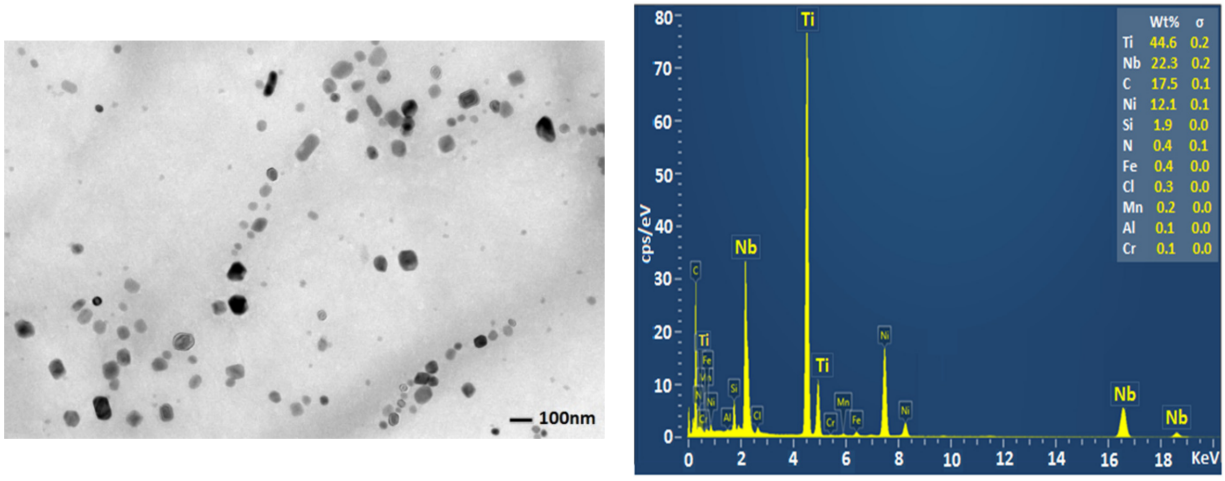

Figure 34. Nb-Ti carbo-nitrides found in a B containing high Al, TWIP tested at 1000 °C, steel 1 in Table 4. The precipitates varied considerably in size (~80 nm in average size) but always gave similar composition. Composition of steel was 0.6% C, 18% Mn, 1.51% Al, 0.033% Nb, 0.075% Ti and 0.011% N. Cooling rate and strain rate were 60 K/min and 3×10^{-3} s^{-1}, respectively [66].

High N levels are therefore beneficial to hot ductility in these B treated TWIP steels, provided there is enough Ti to combine with all the N and the [Ti][N] product is high so that the TiN precipitates out at higher temperatures and so is too coarse to influence ductility [68]. Thus, as can be seen from Figure 30, curve B, the Ti-B TWIP steel, gave the best ductility of the steels examined. A niobium addition of 0.03% to a Ti-B, high N steel may also be important for achieving even better ductility in these TWIP steels. It should be noted that a high Ti addition of 0.1%, which can probably give a significant strengthening of the room temperature yield strength will give satisfactory ductility with or without the Nb addition, curve B in Figure 32.

Hence, presently, for these high Al, Ti-B-treated high Mn TWIP steels of the microalloying additions, V, Ti and Nb, Ti seems to be the best element to add to give both good ductility, Figure 30 and a potentially higher strength at the 0.1% level, Figure 26 [62]. Of

course, there are other requirements that have to be met for the automobile industry, particularly crash ability and high Ti additions can lead to very coarse acicular TiN eutectics which can encourage cracks to develop, resulting in the impact behaviour deteriorating [70]. Clearly, there is further work required before any definitive conclusion can be drawn.

12. Summary and Conclusions

1. P and S are generally detrimental to the hot ductility of both TRIP and TWIP steels, although high P additions have on occasion been found to be beneficial in TRIP steels. For TRIP steels, which are low C steels, the drawback of having a high P level is uncertainty in its effect, because controlling the segregation of P is often difficult. If there is too much segregation, a low melting point iron phosphate type phase forms at the boundaries causing intergranular failure on straightening. If the segregation can be controlled, P seems at times to be able to strengthen the boundary region or remove deleterious precipitates such as NbCN by preferentially taking up vacant sites which NbCN needs for precipitating out on. TWIP steels, because they are generally high C, are subject to even more problems with segregation, resulting in the easier formation of the low melting point iron phosphide type of phase and P levels need therefore to be as low as possible $\leq$0.01% P. In the case of S, if the adverse influence on ductility of having a high Al addition is to be controlled, then it is important to have the S level as low as possible <0.01 wt.% so that its favoured nucleation site, MnS inclusions, are scarce. Moreover, for B-treated steels, because B segregates to MnS inclusions in preference to the grain boundaries, in order to obtain the benefit of B strengthening the boundaries, a low S level is required so it can segregate freely to the grain boundaries.
2. Si does not appear to have a marked influence on the hot ductility. In TRIP steels it tends to move the hot ductility trough to higher temperatures because it increases the transformation temperatures (Ar3 and Ae3). This may involve increasing the straightening temperature by about 60 °C for a 1%Si addition to avoid the hot ductility trough. In TRIP steels, Si delays the precipitation of carbides enabling the carbon content in the austenite to increase so forming a very stable retained austenite at room temperature which can transform to martensite when deformed.
3. In TWIP steel, Si lowers the SFE and therefore encourages dynamic recrystallization as well as encouraging twinning. Because TWIP steels have no hot ductility trough, Si is not likely to influence the hot ductility.
4. Al, by forming AlN, will seriously impair ductility in TRIP and TWIP steels if it forms at the austenite grain boundaries, which is its common location. However, it is needed as a high addition in the composition of these steels for a number of reasons (a) high Al additions can strengthen the room temperature yield strength and so reduce the weight of steel this having become so important for the automobile industry. (b) Al has the ability to prevent delayed hydrogen cracking which is a serious problem for high strength steels. (c) for TWIP steels it encourages twinning, and (d) like Si in TRIP steels, it delays precipitation of carbides but more importantly it can substitute for Si, which gives unsightly stains on the surface of the steel when hot dip galvanised.
5. In TWIP steels, when a high Al level is present in order to be able to cast them satisfactory without cracking B needs to be added and protected from combining with N to form a nitride by a Ti addition.
6. Of the microalloying elements, Nb, Ti and V, which can be used to strengthen high Al, B treated TWIP steels at room temperature, probably Ti will give the best combination of hot ductility and room temperature strength but more work is required to confirm this. This would include impact testing for crashability as a high level of Ti ~0.075–0.1% combined with a high N content (0.01% N) would be needed and this may cause problems with the impact performance. Nb appears to give poor room temperature strength but good ductility as long as there is a high N level, whereas V can achieve a reasonable increase in room temperature strength at the 0.3–0.5% V level but this is

likely to give a poor hot ductility. A lower V level of 0.2% may just possibly be suitable but more work is required to investigate this. A Nb addition of 0.03% combined with a high N content in a B-Ti treated high Al, TWIP steel may also be suitable. Clearly, further work is needed to find the most suitable composition to fulfil all the potentials of these high strength steels.

7. For TRIP steels, it is likely that if the RA value exceeds 35–40% at the base of the hot ductility trough, i.e., before DRX occurs, cracking is unlikely to occur. For TWIP steels, because DRX does not occur during straightening, if the RA value is not in excess of 40% at 700 °C, the lowest temperature of the straightening temperature range, there is likely to be cracking at higher temperatures, as in the absence of DRX, GBS dominates the ductility.

Author Contributions: Conceptualization, B.M.; methodology, B.M.; software, B.M. and A.Q.; validation, B.M.; formal analysis, B.M.; investigation, B.M.; data curation, B.M.; writing—original draft preparation, B.M., A.Q.; writing—review and editing, B.M., A.Q.; visualization, B.M., A.Q.; supervision, B.M.; project administration, B.M. All authors have read and agreed to the published version of the manuscript.

Funding: This research received no external funding.

Institutional Review Board Statement: Not applicable.

Informed Consent Statement: Not applicable.

Data Availability Statement: The data presented in this study are available in the article.

Conflicts of Interest: The authors declare no conflict of interest.

References

1. Hernandez, V.; Mostaghel, S.; Ge, S.; Harris, C.; Cramer, M. Innovative and economical approach for the production of mid-and high-manganese steel. In *AIS Technology Conference Proceedings*; AIS: Pittsburgh, PN, USA, 2016. Available online: https://www.researchgate.net/profile/Sa-Ge-2/publication/309589886_Innovative_and_Economical_Approach_for_the_Production_of_Mid-_and_High-Manganese_Steel/links/5818b4bf08ae1f34d24aa28a/Innovative-and-Economical-Approach-for-the-Production-of-Mid-and-High-Manganese-Steel.pdf (accessed on 1 January 2022).
2. De Cooman, B.C. Chapter 11: High Mn TWIP steel and medium Mn steel. In *Automotive Steels*; Elsevier Ltd.: Amsterdam, The Netherlands, 2017; p. 317.
3. Kim, S.K.; Cho, J.W.; Kwak, W.J.; Kim, G.; Kwon, O. Development of TWIP steel for automotive application. In Proceedings of the 3rd International Steel Conference on New Developments in Metallurgical Process Technologies, Düsseldorf, Germany, 11–15 June 2007; pp. 690–697.
4. Horvath, C.D. Advanced steels for lightweight automotive structures. In *Materials, Design and Manufacturing for Lightweight Vehicles*; Woodhead Publishing: Sawston, UK, 2021; pp. 39–95.
5. De Cooman, B.C.; Chin, K.G.; Kim, J. High Mn TWIP steels for automotive applications. *New Trends Dev. Automot. Syst. Eng.* **2011**, *1*, 101–128.
6. Shi, G.; Westgate, S.A. Techniques for improving the weldability of TRIP steel using resistance spot welding. In Proceedings of the 1st International Conference of the High Strength Steel, Rome, Italy, 2–4 November 2005; pp. 1–13. Available online: http://www.phase-trans.msm.cam.ac.uk/2005/LINK/89.pdf (accessed on 1 January 2022).
7. Zhang, M.; Li, L.; Fu, R.-Y.; Zhang, J.-C.; Wan, Z. Weldability of Low Carbon Transformation Induced PlasticitySteels. *J. Iron Steel Int.* **2008**, *15*, 87.
8. Mintz, B. Hot Dip Galvanising of transformation induced plasticity and other intercritically annealed steels. *Int. Mater. Rev.* **2001**, *46*, 169–197. [CrossRef]
9. UCI Department of Chemistry. Hexagonal Close-Packed Structure. Available online: https://www.chem.uci.edu/~{}lawm/263%202.pdf (accessed on 1 January 2022).
10. Shih, M.; Miao, J.; Mills, M.; Ghazisaeidi, M. Stacking fault energy in concentrated alloys. *Nat. Commun.* **2021**, *12*, 3590. [CrossRef] [PubMed]
11. Monsalve, A.; Barbieri, F.; Gómez, M.; Artigas, A.; Carvajal, L.; Sipos, K.; Bustos, O.; Perez Ipiña, J.E. Mechanical Behavior of a Twip Steel (Twinning Induced Plasticity). *Rev. Mater.* **2015**, *20*, 653–658. [CrossRef]
12. Zambrano, O.A. Stacking fault energy maps of Fe–Mn–Al–C–Si steels: Effect of temperature, grain size, and variations in compositions. *J. Eng. Mater. Technol.* **2016**, *138*, 1–9. [CrossRef]
13. Grässel, O.; Krüger, L.; Frommeyer, G.; Meyer, L.W. High strength Fe–Mn–(Al, Si) TRIP/TWIP steels development–properties–application. *Int. J. Plast.* **2000**, *16*, 1391–1409. [CrossRef]

14. Sato, K.; Ichinose, M.; Hirotsu, Y.; Inoue, Y. Effects of deformation induced phase transformation and twinning on the mechanical properties of austenitic Fe–Mn–Al alloys. *ISIJ Int.* **1989**, *29*, 868–877. [CrossRef]
15. Kim, J.K.; Kim, J.Y. Manufacturing process of ultra high strength steel sheet with the characteristics of excellent ductility. In *Recent Development of Rolling and Following Process Technology and/or Application of Steel Products*; South East Asia Iron & Steel Institute: Shah Alam, Malaysia, 1995; p. 2.
16. Australian Steel Institute. Galvanized Coating Defects in Ingal Specifiers Manual. pp. 78–84. Available online: https://www.steel.org.au/ (accessed on 1 January 2022).
17. Mintz, B.; Yue, S.; Jonas, J.J. Hot ductility of steels and its relationship to the problem of transverse cracking during continuous casting. *Int. Mater. Rev.* **1991**, *36*, 187–220. [CrossRef]
18. Mintz, B. The influence of composition on the hot ductility of steels and to the problem of transverse cracking. *ISIJ Int.* **1999**, *39*, 833–855. [CrossRef]
19. Mintz, B.; Crowther, D.N. Hot ductility of steels and its relationship to the problem of transverse cracking in continuous casting. *Int. Mater. Rev.* **2010**, *55*, 168–196. [CrossRef]
20. Banks, K.M.; Tuling, A.; Klinkenberg, C.; Mintz, B. The influence of Ti on the hot ductility of Nb containing HSLA steels. *Mater. Sci. Technol.* **2011**, *27*, 537–545. [CrossRef]
21. Mintz, B.; Qaban, A. Understanding the high temperature side of the hot ductility curve for steels. *Mater. Sci. Technol.* **2021**, *37*, 237–249. [CrossRef]
22. Kang, S.E.; Kang, M.H.; Mintz, B. Influence of vanadium, boron and titanium on hot ductility of high Al TWIP steels. *Mater. Sci. Technol.* **2020**, *37*, 42–58. [CrossRef]
23. Mintz, B.; Kang, S.; Qaban, A. The influence of grain size and precipitation and a boron addition on the hot ductility of a high Al, V containing TWIP steels. *Mater. Sci. Technol.* **2021**, *37*, 1035–1046. [CrossRef]
24. Liu, Q.; Zhou, Q.; Venezuela, J.; Zhang, M.; Wang, J.; Atrens, A. A review of the influence of hydrogen on the mechanical properties of DP, TRIP, and TWIP advanced high-strength steels for auto construction. *Corros. Rev.* **2016**, *34*, 127–152. [CrossRef]
25. Yin, H. Inclusion characterization and thermodynamics for high-Al advanced high-strength steels. *Iron Steel Technol.* **2006**, *3*, 64–73.
26. Kang, S.E.; Tuling, A.; Lau, I.; Banerjee, J.R.; Mintz, B. The hot ductility of Nb/V containing high Al, TWIP steels. *Mater. Sci. Technol.* **2011**, *27*, 909–915. [CrossRef]
27. Kang, S.E.; Banerjee, J.R.; Tuling, A.S.; Mintz, B. Influence of B on hot ductility of high Al, TWIP steels. *Mater. Sci. Technol.* **2014**, *30*, 486–494. [CrossRef]
28. Tuling, A.; Banerjee, J.R.; Mintz, B. Influence of peritectic phase transformation on hot ductility of high aluminium TRIP steels containing Nb. *Mater. Sci. Technol.* **2011**, *27*, 1724–1731. [CrossRef]
29. Wilson, F.G.; Gladman, T. Aluminium nitride in steel. *Int. Mater. Rev.* **1988**, *33*, 221–286. [CrossRef]
30. Kang, S.E.; Tuling, A.; Banerjee, J.R.; Gunawardana, W.D.; Mintz, B. Hot ductility of TWIP steels. *Mater. Sci. Technol.* **2011**, *27*, 95–100. [CrossRef]
31. Kang, S.E.; Tuling, A.; Banerjee, J.R.; Mintz, B. The hot ductility of TWIP steels. In Proceedings of the 2nd International Conference Super-High Strength Steels, Peschiera del Garda, Italy, 17–20 October 2010.
32. Liu, H.; Liu, J.; Wu, B.; Shen, Y.; He, Y.; Ding, H.; Su, X. Effect of Mn and Al contents on hot ductility of high alloy Fe-xMn-C-yAl austenite TWIP steels. *Mater. Sci. Eng. A* **2017**, *708*, 360–374. [CrossRef]
33. Salas-Reyes, A.E.; Majia, I.; Bedolla-Jacuinde, A.; Boulaajaj, A.; Calvo, J.; Cabrera, J.M. Hot ductility Behaviour of high Mn austenitic Fe-22Mn-1.5Al-1.5 Si -0.45C TWIP steels microalloyed with Ti and V. *Mater. Sci. Eng. A* **2014**, *611*, 77–89. [CrossRef]
34. Mejia, I.; Salas-Reyes, A.E.; Calvo, J.; Cabrera, J.H. Effect of Ti and B microadditions on the hot ductility behaviour of a High-Mn austenitic Fe-23Mn-1.5 Al-1.3Si-0.5C TWIP steel. *Mater. Sci. Eng. A* **2015**, *648*, 311–329. [CrossRef]
35. Banerji, S.K.; Morral, J.E. Boron in steel. In Proceedings of the International Symposium on Boron Steels Held at the Fall Meeting of the Metalurgical Society of AIME, Milwaukee, WI, USA, 18 September 1979. Available online: https://lib.ugent.be/en/catalog/rug01:000098938 (accessed on 1 January 2022).
36. López-Chipres, E.; Mejía, I.; Maldonado, C.; Bedolla-Jacuinde, A.; Cabrera, J.M. Hot ductility behavior of boron microalloyed steels. *Mater. Sci. Eng. A* **2007**, *460*, 464–470. [CrossRef]
37. Salas-Reyes, A.E.; Altamirano-Guerrero, G.; Chávez-Alcalá, J.F.; Barba-Pingarrón, A.; Figueroa, I.A.; Bolarín-Miró, A.M.; Jesús, S.D.; Deaquino-Lara, R.; Salinas, A. Influence of boron content on the solidification structure, magnetic properties and hot mechanical behavior in an advanced as-cast TWIP steel. *Metals* **2020**, *10*, 1230. [CrossRef]
38. Zarandi, F.; Yue, S. The effect of boron on hot ductility of Nb-microalloyed steels. *ISIJ Int.* **2006**, *46*, 591–598. [CrossRef]
39. Mejía, I.; Bedolla-Jacuinde, A.; Maldonado, C.; Cabrera, J.M. Hot ductility behavior of a low carbon advanced high strength steel (AHSS) microalloyed with boron. *Mater. Sci. Eng. A* **2011**, *528*, 4468–4474. [CrossRef]
40. Yamamoto, K.; Suzuki, H.G.; Oono, Y.; Noda, N.; Inoue, T. Formation mechanism and prevention method of facial cracks of continuously cast steel slabs containing boron. *Tetsu-Hagane* **1987**, *73*, 115–122. [CrossRef]
41. Cho, K.C.; Mun, D.J.; Kim, J.Y.; Park, J.K.; Lee, J.S.; Koo, Y.M. Effect of boron precipitation behavior on the hot ductility of boron containing steel. *Metall. Mater. Trans. A* **2010**, *41*, 1421–1428. [CrossRef]
42. Wang, W.S.; Zhu, H.Y.; Sun, J.; Lei, J.L.; Duan, Y.Q.; Wang, Q. Thermodynamic analysis of BN, AlN and TiN precipitation in boron-bearing steel. *Metalurgija* **2019**, *58*, 199–202.

43. Abushosha, R.; Comineli, O.; Mintz, B. Influence of Ti on hot ductility of C–Mn–Al steels. *Mater. Sci. Technol.* **1999**, *15*, 278–286. [CrossRef]
44. Banks, K.M.; Tuling, A.; Mintz, B. Influence of V and Ti on hot ductility of Nb containing steels of peritectic C contents. *Mater. Sci. Technol.* **2011**, *27*, 1309–1314. [CrossRef]
45. Jahazi, M.; Jonas, J.J. The non-equilibrium segregation of boron on original and moving austenite grain boundaries. *Mater. Sci. Eng. A* **2002**, *335*, 49–61. [CrossRef]
46. Cao, B.; Wang, X.; Cui, H.; He, X. Non-equilibrium segregation of boron on grain boundary in Fe-30% Ni alloy. *Int. J. Miner. Metall. Mater.* **2002**, *9*, 347–351.
47. Cameron, T.B.; Morral, J.E. The solubility of boron in iron. *Metall. Trans. A* **1986**, *17*, 1481–1483. [CrossRef]
48. Steenken, B.; Rezende, J.L.L.; Senk, D. Hot ductility behaviour of high manganese steels with varying aluminium contents. *Mater. Sci. Technol.* **2017**, *33*, 567–573. [CrossRef]
49. Kang, S.E.; Banerjee, J.R.; Mintz, B. Influence of S and AlN on hot ductility of high Al, TWIP steels. *Mater. Sci. Technol.* **2012**, *28*, 589–596. [CrossRef]
50. Tanino, M. Precipitation behaviours of complex boron compounds in steel. *Nippon Steel Tech. Rep. Overseas* **1983**, *21*, 331–337.
51. Chen, H.C.; Era, H.; Shimizu, M. Effect of phosphorus on the formation of retained austenite and mechanical properties in Si-containing low-carbon steel sheet. *Metall. Trans. A* **1989**, *20*, 437–445. [CrossRef]
52. Harada, S.; Tanaka, S.; Misumi, H.; Mizoguchi, S.; Horiguchi, H. A formation mechanism of transverse cracks on CC slab surface. *ISIJ Int.* **1990**, *30*, 310–316. [CrossRef]
53. Jiang, X.; Chen, X.M.; Song, S.H.; Shangguan, Y.J. Phosphorus-induced hot ductility enhancement of 1Cr–0.5 Mo low alloy steel. *Mater. Sci. Eng. A* **2013**, *574*, 46–53. [CrossRef]
54. Mintz, B.; Arrowsmith, J.M. Hot-ductility behaviour of C–Mn–Nb–Al steels and its relationship to crack propagation during the straightening of continuously cast strand. *Met. Technol.* **1979**, *6*, 24–32. [CrossRef]
55. Suzuki, H.G.; Nishimura, S.; Imamura, J.; Nakamura, Y. Embrittlement of Steels Occurring in the Temperature Range from 1000 to 600 °C. *Trans. Iron Steel Inst. Jpn.* **1984**, *24*, 169–177. [CrossRef]
56. Mintz, B.; Cowley, A.; Talian, C.; Crowther, D.N.; Abushosha, R. Influence of P on hot ductility of high C, Al, and Nb containing steels. *Mater. Sci. Technol.* **2003**, *19*, 184–188. [CrossRef]
57. Adams, C.J. *Open Hearth and Basic Oxygen Steel Conference: Proceedings, Pittsburgh, PN, USA, 19–21 April 1971*; Iron and Steel Society of the American Institute of Mining: New York, NY, USA, 1971; Volume 54, pp. 290–302.
58. Yashima, Y.; Fujii, M.; Matsumoto, C.; Moriya, T. Effects of Phosphorus Content on High-Temperature Embrittlement of Carbon Steels. *Nisshin Steel Tech. Rep.* **1984**, *51*, 1–7.
59. Kang, S.E.; Banerjee, J.R.; Tuling, A.; Mintz, B. Influence of P and N on hot ductility of high Al, boron containing TWIP steels. *Mater. Sci. Technol.* **2014**, *30*, 1328–1335. [CrossRef]
60. Maehara, Y.; Nagamichi, T. Effects of silicon and nitrogen on hot ductility of low carbon steels. *Mater. High Temp.* **1991**, *9*, 30–34. [CrossRef]
61. Banks, K.M.; Tuling, A.S.; Mintz, B. Influence of chemistry on transverse cracking during continuous casting of medium C high N steel billets. *Mater. Sci. Technol.* **2012**, *28*, 1254–1260. [CrossRef]
62. Scott, C.; Remy, B.; Collet, J.L.; Cael, A.; Bao, C.; Danoix, F.; Malard, B.; Curfs, C. Precipitation strengthening in high manganese austenitic TWIP steels. *Int. J. Mater. Res.* **2011**, *102*, 538–549. [CrossRef]
63. Chateau, J.P.; Dumay, A.; Allain, S.; Jacques, A. Precipitation hardening of a FeMnC TWIP steel by vanadium carbides. *J. Phys. Conf. Ser.* **2010**, *240*, 012023. [CrossRef]
64. Gwon, H.; Kim, J.K.; Shin, S.; Cho, L.; De Cooman, B.C. The effect of vanadium micro-alloying on the microstructure and the tensile behavior of TWIP steel. *Mater. Sci. Eng. A* **2017**, *696*, 416–428. [CrossRef]
65. Kang, S.E.; Banerjee, J.R.; Maina, E.M.; Mintz, B. Influence of B and Ti on hot ductility of high Al and high Al, Nb containing TWIP steels. *Mater. Sci. Technol.* **2013**, *29*, 1225–1232. [CrossRef]
66. Qaban, A.; Mintz, B.; Kang, S.E.; Naher, S. Hot ductility of high Al TWIP steels containing Nb and Nb-V. *Mater. Sci. Technol.* **2017**, *33*, 1645–1656. [CrossRef]
67. Mejía, I.; Salas-Reyes, A.E.; Bedolla-Jacuinde, A.; Calvo, J.; Cabrera, J.M. Effect of Nb and Mo on the hot ductility behavior of a high-manganese austenitic Fe–21Mn–1.3 Al–1.5 Si–0.5 C TWIP steel. *Mater. Sci. Eng. A* **2014**, *616*, 229–239. [CrossRef]
68. Turkdogan, E.T. Causes and effects of nitride and carbonitride precipitation in HSLA steels in relation to continuous casting. In *Steelmaking Conference Proceedings*; AIME: New York, NY, USA, 1987; Volume 70, pp. 399–409.
69. Xu, K.; Mech, S.E. Modelling, heat transfer, precipitate formation and grain growth during secondary spray cooling. In Proceedings of the Continuous Casting Symposium, Annual Report, UIUC, University of Illinois at Urbana-Champaign, Champaign, IL, USA, 5 August 2009.
70. Zhang, L.P.; Davis, C.L.; Strangwood, M. Dependency of fracture toughness on the inhomogeneity of coarse TiN particle distribution in a low alloy steel. *Metall. Mater. Trans. A* **2001**, *32*, 1147–1155. [CrossRef]